

Simulation Based Biarticular and Monoarticular Exoskeletons Design, Analysis, and Comparison

Ali KhalilianMotamed Bonab^{1*}, Volkan Patoglu¹

1 Human Machine Interaction Laboratory, Mechatronics Engineering, Faculty of Engineering and Natural Science, Sabanci University, Istanbul, Turkey.

* alik/vpatoglu@sabanciuniv.edu

Abstract

Introduction

Introduction

The versatility and bipedalism of human locomotion are both unique [1] and the most important characteristics of humans among the mammalian mobility types. While bipedal locomotion has a low energy cost of transport [1], the human versatile musculoskeletal system is not perfectly appropriate for performing all the tasks [2]. For instance, among all movement tasks, two important tasks for human locomotion are running and walking, and it has been proven that running is considerably less efficient than walking [3, 4].

Bipedal locomotion can also lose its efficiency through aging, disease and injury, which can profoundly affect the quality of life [5] due to a loss of independence and mobility. It has been shown that static and dynamic strength [6–8], force development rate [9, 10], prolongation of twitch contraction [7, 11], and passive stiffness [12, 13] of the healthy elderly people's muscles have been remarkably changed compared to those of young, healthy people and consequence of these changes is the weakening the performance of gait [14].

Along with aging, disease and injury are other primary causes of inefficient human locomotion . One of the most important injuries is spinal cord injuries (SCI), which considerably affect the human ability to perform movement tasks [15]. Among all possible diseases causing gait variability, a hemiparetic walking is one of the most and major issues patients face after stroke [16–19]. A stroke can have a serious effect on motor cells and pathways of the central nervous system [17] which can remain after stroke for a long time, restricting patients from reaching normal speed, safe and economical gait [20]; leading to inability on generating desired muscle contraction [17], and generally impaired muscular control [21]. Loss of muscle strength [22], reduced ankle dorsiflexion, and knee flexion [23, 24] are some typical effects of stoke leading to a high cost of transportation on the patient.

Even though in the long term, training can improve the efficiency of locomotion [25] by increasing the stiffness of the tendons [26], and rehabilitation can help patients to achieve near-normal locomotion [20],the muscle and tendon tissues fundamentally constrain the dynamic properties of the muscles and musculoskeletal system compromises between enhancing the efficiency of the desired task and its adaptability [2], and persistence of the neuromotor deficits even after the rehabilitation

constrains [20] the patients from completely resolving the gait issues and reaching complete independence.

By taking advantage of assistive devices not bounded by any fundamental biological limitations, a musculotendon system can be customized to increase the efficiency of performing the desired task while degrading versatility. It can be used for patients to improve their quality of life by modifying their abnormal gait pattern and decreasing their dependency; assistive devices can also be employed to reduce the risk of injuries for tasks needed to carry heavy loads [27–29].

Lower Limb Exoskeletons

The first efforts to develop mobile powered exoskeletons were initiated in 1890 [30]. Despite efforts and progress in accomplishing untethered exoskeleton over a century [31], in 2000 Defense Advanced Research Projects Agency (DARPA) initiated the Exoskeletons for Human Performance Augmentation (EHPA) Program [32], and the first mobile and functional exoskeleton, named Berkeley Lower Extremity Exoskeleton (BLEEX) was developed to augment soldiers' capability of carrying heavy loads over long distances [33]. Sarcos and MIT exoskeletons were introduced [30] after BLEEX as untethered exoskeletons. The same technology with the purpose of assisting impaired populations also was already initiated [34], and ReWalk is one of the well-known exoskeletons [35] which has recently been approved by FDA [36]. The Hybrid Assistive Limbs (HAL) project [37] is another notable project assisting SCI, stroke, and other patients suffering from impaired bipedal walking. Reviews on exoskeletons, prostheses, and orthoses are available in the literature [31, 36–39].

The main objective of assistive devices is reducing the metabolic cost of locomotion and, in particular, decreasing the metabolic energy required for running and walking tasks. Although efforts on designing active exoskeletons to reach this goal were initiated decades ago, the researchers have only recently succeeded in accomplishing this goal [40], which was a tethered device assisting ankle and $6 \pm 2\%$ metabolic cost reduction was reportedly achieved by the ankle exoskeleton. After this exoskeleton, Mooney et al. [41] and Collins et al. [42] reported the reduction of metabolic energy consumption using their ankle exoskeletons. Recently, many exoskeletons and exosuits research groups have reported metabolic cost reduction; a Harvard research group [43] achieved a $32 \pm 9\%$ metabolic burden reduction in post-stroke walking using a tethered exosuit which is one of the notable performance among the performance of exoskeletons developed recently.

Biarticular Actuation

Despite the developments in recent years, a number of challenges need to be surmounted to achieve high metabolic cost reduction to assist people more economically. One of the remarkable challenges on designing an efficient exoskeleton is mass minimization [41, 44, 45] and more importantly, minimizing distal masses [45] has a significant effect on exoskeleton efficiency since adding any mass to the distal extremity will increase the metabolic cost of the locomotion [45] and walking pattern [44]. To address this challenge, using passive exoskeletons without any actuation and power supply module has been proposed; although the metabolic cost reduction is low, they are lightweight assistive devices [42, 46]. An alternative solution is using tethered exoskeletons in which any heavy component is grounded, and actuation is off-board [40, 47]. However, these tethered exoskeletons restrict the mobility of the exoskeleton, and experimental results have been limited to lab-based scenarios.

It has been proven that human bipedal movement is an economical locomotion [1, 48] for various terrains [1, 49] and long distances [50]. It thus inspiration for designing efficient mobile exoskeletons not only to solve the distal mass and inertia problem but

also to provide some additional advantages on the exoskeleton design such as lower power consumption. One of the main reasons for human bipedal locomotion efficiency is the presence of specific muscles, biarticular muscles [51–53], which have several unique and notable roles on human locomotion.

A human lower limb has more muscles than is needed to actuate each degree of freedom(DOF) [53] which means that human lower extremity is redundantly actuated, consisting of monoarticular muscles, which is a type of muscles spanning a joint, and another type span two joints known as biarticular muscles. Although the biarticular muscles, i.e. muscles span two joints, are not necessary for performing movements, they have not been eliminated from the human muscular system during human musculoskeletal system evolution, indicating their advantage for human locomotion [53]. Moreover, the motor control system selects certain muscles to accomplish specific tasks [54], and the metabolic energy consumption is one of the main factors to select muscles to need to be activated among the muscles of desired degrees of freedom [53]. The significance of the biarticular muscles in the energy economy of locomotion has been proven by several computational analyses [55, 56] studying biarticular muscle activation during movement.

The effect of biarticular muscles on locomotion and their benefits have been discussed in multiple studies [51, 53, 57, 58]. One of the key benefits of biarticular muscles is transporting energy from proximal to distal joints produced by monoarticular muscles [51, 59–63]; studies on jumping, which is a high power demanding task, revealed that energy produced by monoarticular muscles at each joint is not sufficient to produce a high jump [59], and energy transportation is necessary to meet the power requirement [59]. Moreover, this proximal to distal energy flow allows for the distribution of the muscles weight, resulting in lower leg inertia [63] which inherently requires less energy to be actuated, leading to more economical locomotion [53, 63]. Elftman [64] also claimed, by studying the running task, that presence of biarticular muscles can regenerate the negative work in phases of running in which adjacent joints have opposite power signs resulting in more economical movement [65] which was confirmed by [66] for walking and jumping as well.

Another central role of biarticular muscles is facilitating the coupling of joint movement [53, 57]; thereby allowing control of the distal joint. For instance, if two joints are coupled with a stiff biarticular muscle, displacement of a joint will cause the movement of another joint as well due to biarticular muscle origin movement [57]. This phenomenon is called ligamentous action [67] which permits the location of most of the monoarticular muscles away from the distal joint and indirectly control them [57]; similar to the energy transportation feature of biarticular muscles, this characteristic of biarticular muscle leads to lower inertia leg [57, 67] which can decrease the metabolic cost of locomotion.

The third remarkable benefit of biarticular muscles is controlling output force direction, which enables to get optimal output power. It has been shown that while most of the work is generated by monoarticular muscles, their output force direction is not optimal [53]. Biarticular muscles are responsible for controlling output force direction [53], which must align with velocity to reach maximum output power [53]. It has also been proven that biarticular muscles have lower contraction velocity than monoarticular muscles [57], resulting in the muscles having concurrent movements [68], and therefore higher muscle force compared to uniarticular muscles [53].

Biarticular muscle effect on limb stiffness has been studied by several researchers [69, 70]; one of the key findings is that loss of stiffness produced by biarticular muscles cannot be compensated by monoarticular muscle stiffness [69, 70]. These studies revealed that the presence of multi-joint muscles would dramatically increase the central nervous system ability to modulate endpoint stiffness [70, 71].

Additionally, biarticular muscle provides necessary coupling to regulate inter-limb interaction [72], and the absence of them would lead to elongated stiffness ellipse, reduce maximum achievable stiffness, and finally limit orientation range [69]. The stability effect of biarticular muscles is another role that has been studied [73–75]. J. McIntyre et al. [73] proved that the presence of biarticular muscles is necessary to provide a coupling enabling passive control of neuro-musculoskeletal system stability.

Considering all these advantages and roles of biarticular muscles in human locomotion, it has inspired the robotics field researchers to adapt their designs to take advantage of biarticular biological features [53]. Several actuators [76, 77], bipedal robots [74, 75, 78], and assistive devices [53] have been designed based on multi-articular muscles configuration. The biarticular component has been used in designing several prostheses trying to mimic gastrocnemius muscle to reduce the actuators energy consumption [79–83] where results represent a promising improvement on the efficiency of prostheses [83]. Several exoskeletons and exosuits are developed also to assist two joints simultaneously [43, 47, 49, 84–86]. Asbeck et al [47] developed a soft exosuit assisting hip and ankle joints using the multi-articular concept on their design and reported 21% to 19% nominal metabolic cost reduction. Another noteworthy soft biarticular exosuit that has been designed for after stroke rehabilitation shows 32% metabolic cost reduction [43]. Quinlivan et al. [85] developed tethered multi-articular soft exosuit, which demonstrated 23% of metabolic burden reduction relative to powered of condition on healthy subject walking. Recently, Xiong et al. [87] proposed a multi-articular passive exoskeleton assisting hip and knee inspired by energy transportation feature of biarticular muscles where it stores negative mechanical work of knee joint and uses to assist hip extension, they succeeded to reduce the metabolic energy consumption by 7.6% without using any actuation module.

Simulation based Analysis of Assistive Devices

Despite all these remarkable progress that have been made on designing exoskeletons and exosuits assisting elderly and disabled subjects suffering impaired gait cycles and healthy individuals, there are remarkable challenges with experimental based studies and designing of exoskeletons. Human in the loop studies always introduce several challenges on interaction with a human, From the establishing experiments perspective, some of the challenges are providing subject-specific prototypes, recruiting appropriate volunteers, guaranteeing their safety during the experiments, and attaining ethic approvals [2]. From physical prototyping viewpoint, collecting information without implementing sensors inside the body in a limited time [2], difficulty or impossibility of some measurements [88], and training effect on subjects performance [89, 90] are some of the important challenges on human in the loop studies and designing procedures.

Simulation-based studies and designing assistive devices can complement the experimental design and analysis to overcome most of the challenges mentioned above. OpenSim is one of the software funded by NIH Roadmap grant U54 GM072970, the NIH research infrastructure grant R24 HD065690, and the DARPA Warrior Web Program and it has been used in movement science related fields [88] and it is getting so attractive for researchers in robotics, biomedical engineering, biophysics, computer science and many other fields [88, 91]. Despite all the limitations on musculoskeletal modeling and simulation [92], OpenSim enables researchers by providing biomechanical models and simulation tools to investigate the human and animals movements [88, 91]. OpenSim has been used to design and study the assistive devices [2, 93–95]. Uchida et al. [2] simulate several combinations of ideal assistive device on subjects running at 2 m/s and 5 m/s speeds and found that activity of muscles can be decreased even in the muscles that do not cross the assisted joints, and it can be increased in some muscles based on assistive device configuration; their simulation results confirmed and proposed

clarification on some of the similar phenomena observed in experimental studies. Several ideal assistive devices effect on the metabolic cost of subjects carrying heavy loads has been studied by Dembia et al. [93], their study like Uchida et al. [2] suggest the effective configurations and joints assist and give a perspective how an assistive device can change muscular activities of subjects carrying loads.

Recently, predictive simulations or simulation-based dynamic optimization approaches are emerging for studying assistive devices which can capture assistive devices effect on the musculoskeletal kinematics and kinetics [96]. This approach has been used by V. Q. Nguyen et al. [97] to study ankle exoskeleton effect on a normal speed walking subject where this approach enables them not only to study the exoskeleton effect on metabolic cost but also to investigate how the exoskeleton affects subject's kinematics and ground reaction forces. A novel active ankle powered prosthesis also was simulated and studied in predictive simulation framework by A. K. Lapre et al. [98]. Predictive simulation has also been employed to simulate knee [99] and ankle prostheses to investigate various control approaches on them [100, 101]. Moreover, Passive ankle prosthesis and Ankle-Foot orthosis stiffness has been optimized using this strategy [102, 103].

Contributions

In this study, biarticular exoskeleton assisting hip and knee has been proposed and compared to another typical monoarticular exoskeleton. To have a methodical insight into the monoarticular and biarticular devices mechanism difference, dynamics and kinematics in motion and velocity level of each device have been derived.

Since the main objective of an exoskeleton is reducing assisted subject's energy expenditure [1] and by considering all the limitations of experimental based studies discussed earlier, we implement the proposed exoskeletons mechanism in musculoskeletal simulation enabling us to not only study the devices but also analyze the musculoskeletal model of the assisted subjects.

This simulation-based study is conducted with ideal exoskeletons where devices have no mass, inertia, or any limiting factor which is beneficial to get insight into how the proposed device can affect the subjects and what is the maximum performance that we can get from the device. Additionally, since every configuration of the exoskeleton can have completely different inertial properties, using ideal exoskeletons allows us to have a fair comparison between monoarticular and proposed biarticular assistive devices.

Although studying the exoskeletons without any restriction on their performance provides handy erudition about the exoskeletons, it is necessary to analyze and compare them in more moderate performance with some constraints. This study introduced a new method to have a legitimate comparison among different configurations of the exoskeletons by taking advantage of Pareto optimization methods and implementing it in the musculoskeletal framework.

This proposed method can provide average optima points for each configuration of the assistive device based on the optimization defined objectives. In this paper, we introduced metabolic cost reduction and devices energy consumption as two optimization criteria and analyzed the devices in lower performance.

The paper is organized as follows: Dynamic Modeling section presents the kinematics and dynamics of the proposed biarticular and the monoarticular exoskeletons mechanism. Musculoskeletal Simulation then addressed the modeling of these assistive devices in OpenSim, simulations procedure, and then Pareto optimization subsection dedicated to explaining the proposed method in detail and its implementation; simulations validation procedure and the results statistical analyses explanation comes after the Pareto optimization simulations subsection. Results and their discussions are provided in the Results and Discussion section mainly separated

into two main subsections, including exoskeletons results in maximum and more moderate performances; study limitation and performance metrics are also provided in this section. Finally, this paper is concluded with Conclusions and Future Work section, which also presents future research directions.

Kinematic Modeling

The biarticular exoskeleton was designed to assist hip and knee joint. The exoskeleton has been inspired by biarticular muscles and the aim of the design was keeping the weight in proximal joint (Hip) while delivering the required power to distal joint (Knee). The parallelogram mechanism has been purposed to accomplish this goal and take advantage of biarticular muscles biological features in the exoskeleton. The purposed exoskeleton was shown in figure 1.

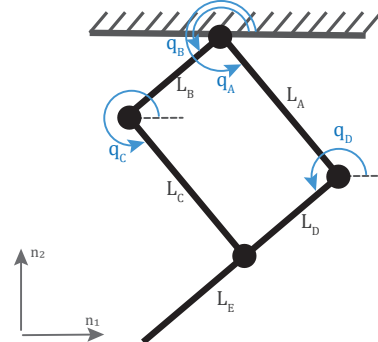


Fig 1. Biarticular exoskeleton design.

Where the hip joint will be assisted by applying directly the torque on the joint and second actuator torque will be applied to knee joint through the parallelogram mechanism where kinematics is

$$x_{Bi} = l_A \cos(q_A) + (l_E + l_D) \cos(q_B) \quad (1)$$

$$y_{Bi} = l_A \sin(q_A) + (l_E + l_D) \sin(q_B) \quad (2)$$

Monoarticular Exoskeleton can be modeled as a two-link serial manipulator as shown in figure 2 where each joint is assisted by the directly joint actuator and the forward kinematics of monoarticular exoskeleton is:

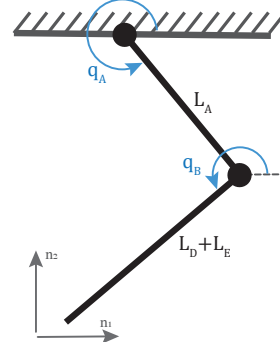


Fig 2. Monoarticular exoskeleton design.

$$x_{mono} = l_A \cos(q_A) + (l_E + l_D) \cos(q_A - q_B) \quad (3)$$

$$y_{mono} = l_A \sin(q_A) + (l_E + l_D) \sin(q_A - q_B) \quad (4)$$

For both of the exoskeletons configurations the kinematics in motion level also can be easily driven and resulted Jacobian of each configurations can be written as in Eq (5) and (6).

$$J_{Bi} = \begin{bmatrix} -l_A \sin q_A & -(l_E + l_D) \sin(q_B) \\ l_A \cos(q_A) & (l_E + l_D) \cos(q_B) \end{bmatrix}_{2 \times 2} \quad (5)$$

$$J_{Mono} = \begin{bmatrix} -l_A \sin q_A - (l_E + l_D) \sin(q_A - q_B) \\ l_A \cos q_A + (l_E + l_D) \cos(q_A - q_B) \\ (l_E + l_D) \sin(q_A - q_B) \\ -(l_E + l_D) \cos(q_A - q_B) \end{bmatrix}_{2 \times 2} \quad (6)$$

As it can be interpreted from the kinematics of exoskeletons, there is a jacobian between monoarticular and biarticular exoskeletons as it is represented in Eqn 7.

$$\begin{aligned} \omega_{2 \times 1, \text{monoarticular}} &= J_{2 \times 2} \omega_{2 \times 1, \text{biarticular}} \\ \begin{bmatrix} \text{torso} & \omega_{\text{mono}}^{\text{femur}} \\ \text{femur} & \omega_{\text{mono}}^{\text{tibia}} \end{bmatrix} &= \begin{bmatrix} 1 & 0 \\ -1 & 1 \end{bmatrix} \begin{bmatrix} \text{torso} & \omega_{\text{bi}}^{\text{femur}} \\ \text{torso} & \omega_{\text{bi}}^{\text{tibia}} \end{bmatrix} \end{aligned} \quad (7)$$

Using Eqn 7 which is a mapping between the angular velocities of the exoskeletons, we can derive the mapping between the provided torque by exoskeletons.

$$\begin{aligned} \tau_{2 \times 1, \text{biarticular}}^T \omega_{2 \times 1, \text{biarticular}} &= \tau_{2 \times 1, \text{monoarticular}}^T \omega_{2 \times 1, \text{monoarticular}} \\ \tau_{2 \times 1, \text{biarticular}}^T \omega_{2 \times 1, \text{biarticular}} &= \tau_{2 \times 1, \text{monoarticular}}^T J \omega_{2 \times 1, \text{monoarticular}} \end{aligned}$$

Rewriting the equations more clearly, we can express the torque mapping explicitly as Eqn.8.

$$\begin{aligned} \tau_{2 \times 1, \text{biarticular}} &= J^T \tau_{2 \times 1, \text{monoarticular}} \\ \begin{bmatrix} \tau^{\text{torso/femur}}_{\text{bi}} \\ \tau^{\text{torso/tibia}}_{\text{bi}} \end{bmatrix} &= \begin{bmatrix} 1 & 0 \\ -1 & 1 \end{bmatrix}^T \begin{bmatrix} \tau^{\text{torso/femur}}_{\text{mono}} \\ \tau^{\text{femur/tibia}}_{\text{mono}} \end{bmatrix} \end{aligned} \quad (8)$$

This relation between two exoskeleton has been used to verify the modeling of the exoskeleton through musculoskeletal simulation framework.

Musculoskeletal Simulation

Musculoskeletal Model

The exoskeletons have been studied through musculoskeletal simulations by conducting the simulations of the seven subjects walking normally and while carrying a 38kg load on the torso at their chosen speed. The data that has been used in this study was experimentally collected and processed by Dembia et.al. [93] and their experimental protocol was approved by the Stanford University Institutional Review Board [93].

The musculoskeletal model used in the simulations, which was the same with the model used by dembia et al. [93], was a three-dimensional model developed by Rajagopal et al. [104] with 39 degrees of freedom where the lower limbs were actuated using 80 massless musculotendon actuators, and the upper limb actuated by 17 torque actuators [104].

This three-dimensional musculoskeletal model was adapted by locking some unnecessary degrees of freedom for both normal walking and walking with a heavy load scenarios and modeling the extra load on the torso of the musculoskeletal model for the walking with heavy load condition [93].

Since this research was built upon the study performed by Dembia et al., we will follow the similar terminologies in most of the cases to avoid any confusion for the readers. Therefore, the loaded condition will refer to the subjects walking while carrying the 38Kg load on their torso while the noload condition will reference the subjects walking without any extra load at their self chosen speed.

Simulation Procedure

The first step for conducting the simulation of the specific subject is scaling the generic dynamic model to acquire a musculoskeletal model matching with the anthropometry of the subject which was performed using OpenSim Scale Tool and according to the mass and height of the subject, the maximum isometric forces of the muscles were scaled. After obtaining the specific model for the subject, inverse kinematics of the subject were computed using OpenSim Inverse Kinematics Tool and the motion capture data collected experimentally.

On the next stage of the simulation workflow, the scaled model, inverse kinematics and ground reaction forces were employed to run the RRA algorithm [91]. The RRA algorithm reduces the incompatibility of experimental data including ground reaction forces and trace data and musculoskeletal model by slightly adjusting inertial properties and kinematics. Then adjusted model and kinematics generated by RRA were employed to perform muscle driven simulations using Computed muscle control algorithm in OpenSim [105].

Computed Muscle Control (CMC) algorithm simulates the muscle recruitment of the subject by resolving muscle redundancy problem using static optimization to find the required muscle excitations to track the provided kinematics. The CMC simulations output were then used to run the analysis tool of OpenSim to compute subjects metabolic power consumption, and muscles moment.

The figure 3 demonstrates the workflow of the simulation in OpenSim in which green blocks stands for output, blue blocks are OpenSim simulations or analyses, purple blocks are models that have been used for simulations and analyses, and finally, red blocks represent processed experimental data.

The OpenSim solves the muscle redundancy problem to track experimentally measured motion and uses effort-based objective, as Eqn. 9, to solve for a set of muscle excitations to track measured motions and forces within a specified tolerance using static optimization at each time step during the motion of interest [92]. Therefore, the kinematics and dynamics of the subject will remain consistent during the simulations and any additional mass and inertia on the subject that has not been captured by experiments will cause a systematic error on the results.

$$J = \sum_{i \in nMuscles} a_i^2 + \sum_{i \in nReserves} \left(\frac{\tau_{r,i}}{w_{r,i}} \right)^2 \quad (9)$$

With the knowledge of the OpenSim neural control algorithm, we used the adjusted model and kinematics provided by Dembia et al. [93] instead of reproducing all data from the beginning of the simulation procedure which also helped us to ease the verification of the simulations procedure thanks to [93] for verified simulations data.

Metabolic Model. To calculate the estimation of the instantaneous metabolic power of subjects, Umberger [106] muscle energetic model which was modified by

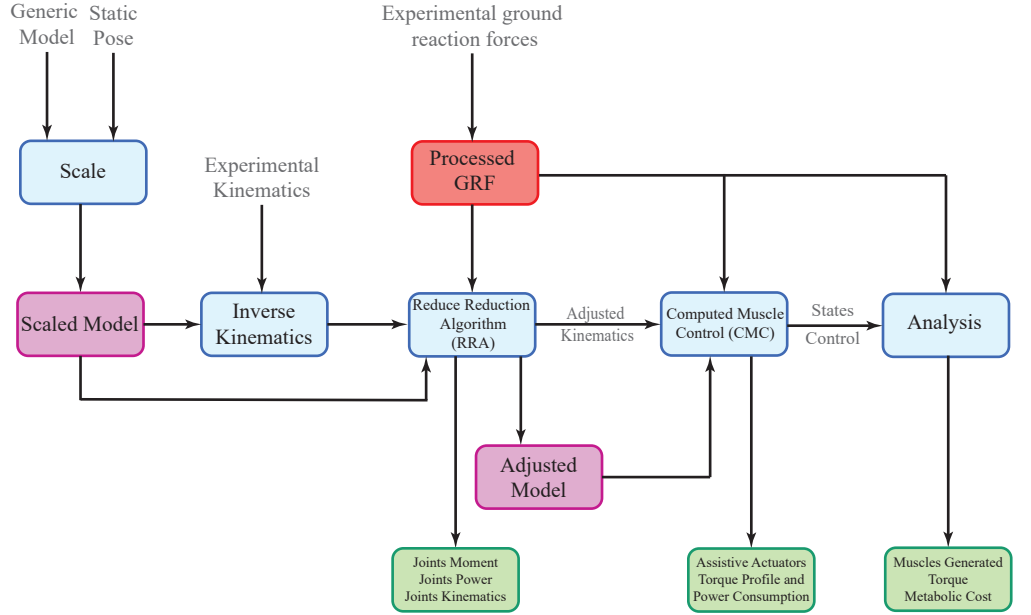


Fig 3. OpenSim simulation procedure block diagram.

Uchida et al. [107] were employed in which average power consumption of a muscle during a gait cycle was calculated using Eq.10 [107].

$$P_{avg} = \frac{m}{t_1 - t_0} \int_{t_0}^{t_1} E(t) dt \quad (10)$$

Where m is muscle mass, and $E(t)$ is the normalized metabolic power consumed. This model generates metabolic power of all muscles and then whole body metabolic power was calculated by summing all muscles metabolic power [107]. For computing the gross metabolic energy consumption of subjects, we integrated the metabolic power over the gait cycle and then divided by the mass of subjects.

As it is mentioned in [93], due to experimental data insufficiency, some subjects and trials simulation were not a complete gait cycle, therefore, the metabolic energy were calculated for a half of a gait cycle for these subjects and trials which is a verified method for computing the energy according to [93].

Modeling and simulation of assisted subjects

The kinematics of the exoskeletons were already discussed and in order to model ideal exoskeletons in OpenSim framework we used the Torque Actuators provided by OpenSim API [91]. Biarticular and Monoarticular exoskeletons' torque actuators were assigned, as shown in figure 4. As it is represented in figure 4 (a), both torque actuators of biarticular exoskeleton were assigned to torso , then, reaction forces of the actuators were applied to the torso which is in the match with the kinematics and dynamics

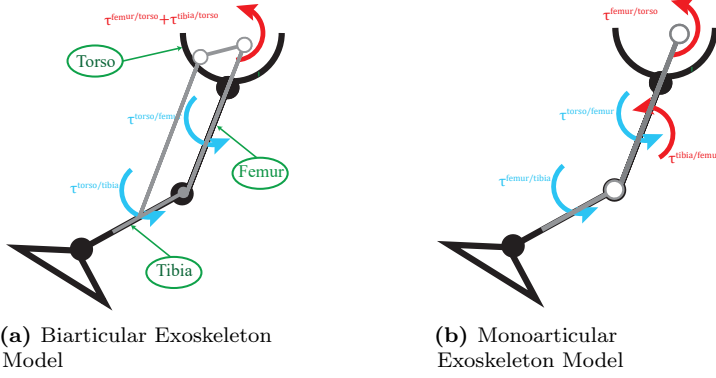


Fig 4. Exoskeletons modeling on OpenSim

model of the biarticular exoskeleton.

$$\tau_{Biarticular}^{hip} = \tau^{torso/femur} \quad (11)$$

$$\tau_{Biarticular}^{knee} = \tau^{torso/tibia} \quad (12)$$

Monoarticular exoskeleton (figure 4 (b)) modeled by assigning hip joint actuator from torso to femur body and knee joint actuator assigned from femur to tibia body where knee torque actuator's reaction torque applied to femur body:

$$\tau_{Monoarticular}^{hip} = \tau^{torso/femur} \quad (13)$$

$$\tau_{Monoarticular}^{knee} = \tau^{femur/tibia} \quad (14)$$

Computed Muscle Control adjusted objective function. To investigate the performance of the assistive devices and their effect on human musculoskeletal system through OpenSim simulation framework we used the CMC algorithm. Computed Muscle Control algorithm objective function depends on the sum of squared muscle activation and reserve actuators, which compensates for modeled passive structures and potential muscle weakness [93]:

$$J = \sum_{i \in nMuscles} a_i^2 + \sum_{i \in nReserves} \left(\frac{\tau_{r,i}}{w_{r,i}} \right)^2 \quad (15)$$

Where w_i determines the weight of reserve actuators which is generally selected as a small number to highly penalize using of reserve actuators. By adding assistive device actuators (i.e. Torque Actuators) to the musculoskeletal model of the subject they will be added to the CMC tool objective function. The adjusted objective function will include the assistive actuators as it is expressed in Eq. (16) and by selecting proper weights for the assistive actuators, they can be chosen by the optimizer as the actuation of the assigned degree of freedom.

$$J = \sum_{i \in nMuscles} a_i^2 + \sum_{i \in nExo} \left(\frac{\tau_{exo,i}}{w_{exo,i}} \right)^2 + \sum_{i \in nReserves} \left(\frac{\tau_{r,i}}{w_{r,i}} \right)^2 \quad (16)$$

In the adjusted objective function, $w_{exo,i}$ is torque actuator weights which is named optimal force in OpenSim [93] penalizing the usage of torque actuators. By selecting a large number, penalization of the actuators will be insignificant and they will be

selected for actuating the joint between two bodies assigned for torque actuator and if we select a small optimal force, the optimizer will highly penalize the usage of exoskeleton actuators. To study each configuration of the exoskeleton in their maximum performance, the assigned torque actuator's optimal force was selected as 1000 N.m enabling the optimizer to use the assistive actuators as much as possible during a gait cycle simulation.

Metabolics and actuators energy calculation. Similar to the unassisted procedure, the instantaneous metabolic power of the subjects was computed using the energetic model of Uchida et al. [107] and then metabolic energy of subjects were derived by integration of the metabolic power over the gait cycle. In order to compute the energy consumption of the assistive actuators, the power profile of the actuators were obtained and their absolute power profiles were integrated over the gait cycle and divided to the subjects mass. Similar to the energy consumption of the exoskeleton procedure, the negative energy or regeneratable energy through a gait cycle were calculated by obtaining the negative power profile and integrated over the gait cycle and normalized to the mass of the subject.

Pareto Optimization Simulations

The optimization stage of the Computed Muscle Control (CMC) algorithm uses the weighted sum of squares to solve muscles and assigned actuators redundancy to select a set of actuation with the lowest cost for tracking the kinematics of the dynamic model of the subject [92]. To investigate the ideal assistive devices maximum effect on the subjects metabolic power consumption regardless of their energy expenditure, large weights were assigned to assistive actuator.

However, in the real-time, exoskeletons are restricted by the energy that can be supplied to the actuation module and the maximum torque that the actuation module can provide to the joint of interest; to study devices performance under the maximum provable torque to the joints and their effect on musculoskeletal system in lower energy consumption regions, we used the Pareto-Optimization concept [108].

Pareto method integrates all optimization criteria in its procedure and constructs a Pareto front representing trade-off among the criteria enabling us to have optima curves for each configuration of the devices [109] and conduct a fair comparison between the exoskeletons and the load conditions. In this study, metabolic cost reduction and assistive actuators energy consumption were considered as two optimization criteria to study the trade-off between the exoskeletons and load conditions.

One of the acceptable Pareto front is a discrete set of Pareto-optima points obtained by constructing a single objective function by integrating objectives and optimizing the single cost function throughout the specific range of values of the parameters used to combine the cost functions into a single objective function [110].

The pareto optimization method has been used by M. L. Handford and M. Srinivasan [100, 101] to study robotic lower limb prostheses by simultaneously optimizing the metabolic and prosthesis cost rate.

The workflow of the Pareto-optimization simulations. To accomplish the simulations of the Pareto-optimization in the OpenSim framework, we constrained the peak torque of assistive actuators constraining the objective function mentioned in Eq 16 throughout a specific range from high to low provable torque throughout a gait cycle changing the solution of the optimizer for muscles and actuator redundancy problem. This variation over the discrete range of maximum provable torque resulting in different points on the optimization objectives space and by filtering points, we achieved to Pareto front for each configuration of the exoskeleton.

For the biarticular and monoarticular exoskeletons in both loaded and noload conditions, the maximum torque of the actuators were varied between 30 N.m and 70 N.m. For performing the simulations, the constraint of the hip actuator was fixed and the constraint of the knee was varied; after simulating all of the exoskeletons with a fixed hip constraint and varying knee constraint, the constraint of the hip actuator was changed for performing the next iteration of the simulations. The algorithm has been shown the following pseudo code.

Algorithm 1 Pareto Simulations Algorithm

```

1: for  $i = [70, 60, 50, 40, 30]$  do
2:   for  $j = [70, 60, 50, 40, 30]$  do
3:     Set  $\{-i, i\}$  : hip actuators constraint:  $\{MinControl, MaxControl\}$ 
4:     Set  $\{-j, j\}$  : knee actuators constraint:  $\{MinControl, MaxControl\}$ 
5:     Update exoskeleton model by the new constraints
6:     Perform CMC Simulation
7:   end for
8: end for

```

Inertial properties of the exoskeletons effect on metabolic rate. One of the main challenges with designing the mobile exoskeletons is the effect of the mass and inertia, grounded on the extremities of the subjects, on the metabolic rate of the subjects. The effect of mass and inertia on the metabolic cost has been studied through several literatures [111, 112] and shown that metabolic rate of the subject would change considerably by adding mass and inertia [111–113].

The proposed exoskeleton in this studies have a remarkable difference from the inertial properties due to their kinematic design and it will result in different effect on the metabolic rate of the subjects.

Since the current neural control algorithm of the OpenSim is not able to simulate adding any mass that has not been captured by experimental data, we simulated the effect of the mass and inertia offline using the metabolic model of the Browning et al. [111] in which they analyzed and proposed linear model for the effect of adding mass and inertia on each segment of lower limbs. In the study accomplished by Browning et al. [111], subjects were walking at 1.25 m/s without carrying any heavy load on their torso which is similar to the data captured from the subjects in the walking with noload at their self selected speed [93].

The mass and inertia of the proposed biarticular and monoarticular exoskeletons affect the waist, thigh and shank segments. As it is discussed in the Kinematic Modeling section, the biarticular exoskeleton, unlike monoarticular one, is designed to deliver the assistance distally to the knee joint.

It enables designers to attach actuation module to the waist instead of thigh meaning that the main difference between inertial properties of two exoskeletons will be on the attached mass on the waist and shank segments nevertheless the reflected inertia of the actuation module will be reflect on the actuated joint regardless of its grounded segment in both exoskeletons.

For the purpose of conducting numerical simulations of the inertial properties of the exoskeletons effect on the subjects metabolic rate, we assigned two identical masses and the center of masses measured from the hip and knee joints for the links attached to the thigh and shank respectively. Additionally,a typical and identical actuation module inertia and mass has been assigned for both configurations of the exoskeleton.

In order to study the effect of the inertia in the pareto simulations, the maximum achievable torque of the actuator has been set to 2 N.m which can be provided by MaxonMotor EC90 Flat 260W and the required transmission ratio is calculated by

diving the peak torque at joint level to peak torque of the actuator and then reflected inertia has been calculated using Eqn.17.

$$R = \frac{\tau_{max,jointlevel}}{\tau_{max,actuator}}$$

$$I_{reflected} = I_{actuator} \times R^2 \quad (17)$$

The inertia of the moving segments (i.e., thigh and shank segments) have been computed by considering the distal mass effect on the inertia, which is different for each configuration of the exoskeletons, reflected inertia of the actuation module and the leg inertia provided by [111] which is calculated about center of rotation of the leg in the body frame. The Eqn.18 represents the inertia calculation of a segment.

$$I_{Exo,segment} = I_{reflected} + m \times COM^2 \quad (18)$$

$$I_{loaded\ leg} = I_{Exo,segment} + I_{noload\ leg}$$

The typical mass, center of mass and inertia that have been used for numerical simulations are represented in Table 1. These values are mostly in match with the mechanical properties of the biarticular and monoarticular exoskeletons designed in our lab.

Table 1. Mass and inertia properties of two typical exoskeletons.

Configuration	Waist	Thigh		Shank		Actuator
	Mass (kg)	Mass ((kg))	COM (m)	Mass ((kg))	COM (m)	Inertia (kg.m ²)
Biarticular	6	1	0.23	0.9	0.18	0.000506
Monoarticular	3	2.5	0.30	0.9	0.18	0.000506

The metabolic model proposed by Browning et al. [111] is calculating the metabolic rate of the subject with loaded segment, however, Since we were interested in the effect of inertial properties of exoskeleton on metabolic rate change, not metabolic rate, we used the model by subtracting the metabolic rate of the subject walking without the additional mass. The equations of the final model that has been used for analyzing the effect of exoskeleton mass and inertia on the metabolic rate is provided in Eqn.19 and 20 respectively.

$$\Delta MC_{Waist} = 0.045 \times m_{Waist}$$

$$\Delta MC_{Thigh} = 0.075 \times m_{Thigh}$$

$$\Delta MC_{Shank} = 0.076 \times m_{Shank} \quad (19)$$

$$I_{ratio} = \frac{I_{Exo,segment} + I_{unloaded\ leg}}{I_{unloaded\ leg}}$$

$$\Delta MC_{Thigh} = ((-0.74 + (1.81 \times I_{Thigh,ratio})) \times MC_{unassisted}) - MC_{unassisted}$$

$$\Delta MC_{Shank} = ((0.63749 + (0.40916 \times I_{Shank,ratio})) \times MC_{unassisted}) - MC_{unassisted} \quad (20)$$

Validation of Simulations

The comprehensive validation procedure of the OpenSim simulations was published by the Hicks et al. [92] where they explained how to validate modeling and simulation results at each stage. Additionally, Dembia et al. [93] explained simulation verification for their assistive device simulations and we followed the same procedures explained in [92, 93] to validate our results from the simulations.

As it is already discussed, the adjusted model, adjusted kinematics and processed ground reaction forces that has been provided by [93] have been used for accomplishing this study which has been evaluated and validated by Dembia et al. [93]. As it is recommended in [92], the muscular activation resulted from the simulation has been validated with the experimentally recorded electromyography (EMG) signals.

The loaded and noload joint kinematics and kinetics were compared with the results of the studies accomplished by Huang and Kuo [114] and Silder et al. [115] and validated qualitatively. Since our simulations of the unassisted subject for loaded and noload conditions were the same with Dembia et al. simulations, we reproduced their simulations and compared them with their results to validate our reproduced simulations results. Additionally, since we used the provided RRA results for performing the CMC simulations, the joint moment and joint kinematics represented in this paper were already validated.

The other source of error during the simulations are kinematics and residual errors which were analyzed to be in the recommended thresholds [92]; nevertheless, since the inverse kinematics stage of simulation was not reproduced in this study, the markers error was not examined. Another error source in these simulations could be additional moments introduced to compensate any modeled passive structures and muscles weakness where it is recommended to have less than 5% of net joint moments in peak and RMS [92]. It has been checked for all simulations and confirmed that the reserve actuator torques are smaller than the recommended percentage of joint moments.

Performance Metrics

For the purpose of having methodical analysis and comparison between the assistive devices and load conditions some performance metrics have been defined. As discussed earlier, the ultimate goal of each assistive device is reducing energy consumed by the subject for performing a task which is walking with and without load at normal speed in this study. Therefore, we calculated the normalized gross whole-body metabolic rate of the subjects in two different assistive devices and load conditions and then metabolic cost reduction has been computed using the metabolic rate of assisted and unassisted subjects. This procedure of metabolic cost calculation was repeated for all seven subjects in three trials to obtain the total average metabolic energy expenditure and metabolic cost reduction for each assistance scenario and load condition.

Another important metrics for assessing the performance of an exoskeleton is the energy it consumes to provide the assistance. To analyze this metrics in the simulated exoskeletons, we computed the absolute energy consumed by the all actuators and the reason for considering the absolute value is absence of the regeneration mechanism as a general case for the exoskeletons. On the other hand, in order to analyze the amount of energy available for regeneration, we computed the negative energy of the exoskeletons. This metric is a crucial part of the untethered exoskeletons analysis to estimate the battery life.

At the pareto optimization part of the study, these two metrics (i.e., metabolic cost reduction and energy consumption) are represented together by averaging them for each defined constraints over the subjects and represented with mean and standard deviation for both criteria. This metric represents the set of different configurations for each exoskeleton in terms of energy consumption and the amount of assist the device can provide. For more detailed analyses, some specific configurations in each exoskeleton and load condition have been selected and compared in more comprehensive manner.

Finally, some of the muscular activations of the lower limb key muscles were extracted and studied to have insight into how an assistive device can change muscles activities and consequently, metabolic cost which is resulted from muscles activities.

Statistical Analysis

To have systematic comparisons among each scenario, we set statistical analyses for the results of assisted and unassisted subject simulations. Two main objectives in this study were the effect of exoskeleton on human metabolic cost and the exoskeletons' power consumption where they need to be tested among scenarios to study if there is any statistically significant difference among the assistance scenarios or not. Since the simulations were done on seven subjects with three trials in five different scenarios, repeated measures analysis of variance (ANOVA) and Tukey Post-hoc were employed for statistical analyses. Additionally, for each represented profile, mean and standard deviations were calculated and represented in figures.

Results and Discussion

Ideal Exoskeletons with Maximum Performance Musculoskeletal Simulations Results

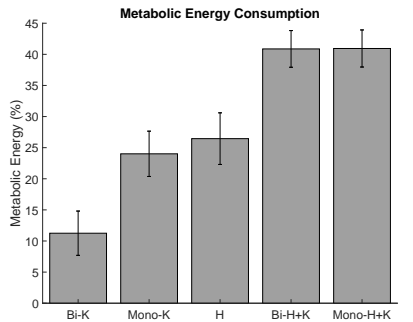
Device Performance

All five configurations of ideal exoskeletons with maximum Optimal Force (i.e. 1 MN.m) decreased the metabolic cost of subjects running at 2 m/s compared with running subjects without any assistance. Biarticular and monoarticular knee exoskeletons reduced $11.25 \pm 3.64\%$ and $24.01 \pm 3.55\%$ metabolic energy, and hip exoskeleton reduced the subject energy consumption by $26.45 \pm 4.34\%$, two main configurations of the exoskeleton had the most significant reduction in the metabolic energy where biarticular and monoarticular exoskeletons reduced the running subjects lower extremity's muscle energy by $41.23 \pm 3.04\%$ and $41.21 \pm 3.04\%$. These results are matching with Uchida et al. [2], which they used the same dataset to perform their simulations. As it can be inferred from the average metabolic energy reduction, monoarticular knee exoskeleton has better performance than biarticular one when they are assisting knee joint, however, metabolic cost reduction on the main exoskeletons are almost the same. Figure 5a represents metabolic energy reduction by five different configurations of exoskeletons when subjects were running in 2 m/s speed.

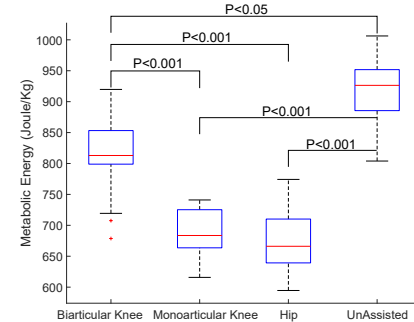
Among the exoskeletons assisting a joint, hip exoskeleton has the highest positive peak and mean power resulting in a significantly lower metabolic cost to peak/mean positive power ratio (Table 2 and 3). Although biarticular knee exoskeleton provides low assistance to subjects, its power consumption is also considerably low such that metabolic to peak and mean power ratios are highest among all the exoskeletons assisting a joint. Between monoarticular and biarticular exoskeletons assisting hip and knee joints, hip actuators have very similar power consumption and ratios; however, biarticular exoskeleton's knee actuator has considerably better performance such that it has remarkably lower peak and mean power which causing to higher metabolic power to peak/mean power ratios. Tables 2 and 3 give a broad view of the torque profiles of five different configurations of the exoskeleton which is reported as a mean \pm standard deviation across seven subjects.

Devices Power and Torque

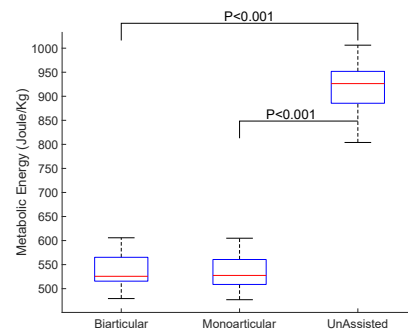
During a gait cycle, all five configurations of the exoskeleton had different torque profiles than the assigned joint moment, which is the same with relevant papers [2, 93]. The assistive devices are primarily active during stance phases, and all of them reached their peak moment during the mid-stance phase.



(a) Assisted subjects lower extremity muscles average metabolic energy reduction.



(b) Single joint assistive devices effect on metabolic energy expenditure of the subjects



(c) Monoarticular and biarticular assistive devices effect on metabolic energy expenditure of the subjects

Fig 5. Ideal exoskeletons effect on the 7 running subjects energy consumption.

According to figure 7(b) and 7(d), biarticular knee exoskeleton neither follow hip nor knee joint moment during a gait cycle and increasing the muscles generated moment to compensate for opposing torque which needs to increase the subjects metabolic cost. However, since optimizer used the device to reduce overall muscle activation this is the optimal profile for the biarticular exoskeleton.

Similar phenomena where muscles generated moments and assistive device torques are opposing with each other can be seen in other configurations of the exoskeletons assisting a joint as well which is selected as an optimal torque profile by Computed Muscle Control algorithm. This behavior will be analyzed in the "Device Effect on Muscles Activation and Generated Moment".

Figure 7(d)-(a) demonstrates the torque profiles for two main configurations i.e. Monoarticular and Biarticular exoskeletons assisting hip and knee. Biarticular exoskeleton knee actuator's torque is completely different from biarticular knee exoskeleton profile while the monoarticular exoskeleton in both hip and knee actuators torque profiles are similar to hip and monoarticular knee exoskeletons. In a gait cycle, monoarticular and biarticular devices are opposing the joint moment and muscles generated moment during some phases of the gait cycle which is more evident in hip actuators where it opposes the muscles considerably during stance and swing phases.

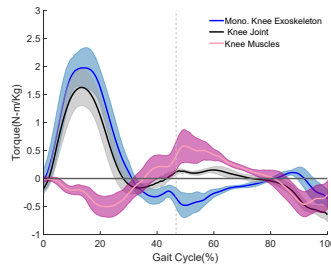
Furthermore, while exoskeletons have similar torque profiles, the monoarticular hip actuator executes more torque than biarticular one (Table 2) which is already expected

Table 2. Ideal exoskeletons torque data and performance

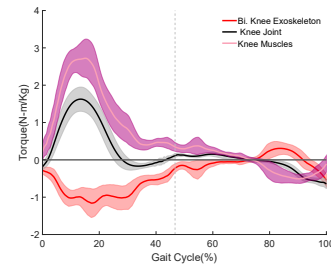
Device	Actuator	Peak Torque (N-m/Kg)	Mean Positive Torque (N-m/Kg)	Mean Negative Torque (N-m/Kg)	Metabolic Power to Peak Power Ratio	Metabolic Power to Mean Positive Power Ratio
Monoarticular Hip+Knee	Total					
	Hip Actuator	-2.57±0.50	0.23±0.07	-0.57±0.12	0.52±0.12	2.84±0.66
Biarticular Hip+Knee	Knee Actuator	1.29±0.30	0.22±0.06	-0.14±0.02	1.58±0.59	7.73±2.52
	Total					
Biarticular Knee	Hip Actuator	-2.5±0.43	0.23±0.07	-0.55±0.11	0.54±0.12	2.91±0.71
	Knee Actuator	1.29±0.30	0.22±0.06	-0.14±0.02	2.03±0.62	10.84±2.95
Biarticular Knee		0.40±0.17	0.3±0.02	-0.41±0.07	2.05±0.38	7.71±0.98
Monoarticular Knee		2.05±0.33	0.37±0.07	-0.14±0.02	1.32±0.27	6.40±0.92
Hip		-2.64±0.60	0.25±0.06	-0.55±0.12	0.64±0.16	3.36±0.76

Table 3. Ideal exoskeletons power, energy consumption and metabolic power.

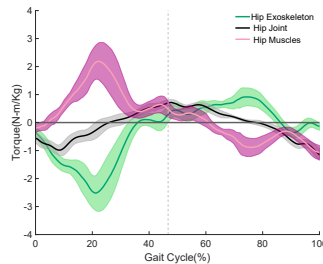
Device	Actuator	Mean Metabolic Power (W/kg)	Peak Positive Power (W/kg)	Mean Positive power (W/kg)	Mean Negative Power (W/kg)	Mean Energy (J/kg)	Regeneratable Energy (J/kg)
Monoarticular Hip+Knee	Total	5.36 ± 0.36					
	Hip Actuator		10.68 ± 2.28	1.97 ± 0.43	-0.17±0.08	216.33±47.54	18.65±8.16
Biarticular Hip+Knee	Knee Actuator		4.06 ± 2.22	0.77 ± 0.28	-0.52±0.09	131.06±33.65	53.48±10.35
	Total	5.36 ± 0.37					
Biarticular Hip+Knee	Hip Actuator		10.35 ± 2.15	1.93 ± 0.51	-0.18±0.08	211.38±45.17	18.17±7.76
	Knee Actuator		2.91 ± 1.04	0.52 ± 0.13	-0.53±0.10	106.89±22.79	54.24±13.90
Biarticular Knee		8.13±0.58	4.08±0.81	1.06±0.12	-0.05±0.02	112.17±14.02	5.59±2.97
Monoarticular Knee		6.87±0.36	5.43±1.23	1.10 ± 0.19	-0.59±0.15	169.74±26.44	59.51±15.85
Hip		6.72±0.53	10.92±2.37	2.08±0.45	-0.14±0.05	222.99±46.50	14.12±5.41



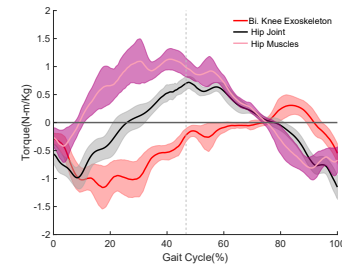
(a) monoarticular knee exoskeleton actuator torque profile.



(b) Biarticular knee exoskeleton actuator torque profile.



(c) Hip exoskeleton actuator torque profile.



(d) Biarticular knee exoskeleton actuator torque profile.

Fig 6. Exoskeletons assisting a joint torque profiles compared to net joint moment and muscles generated moment.

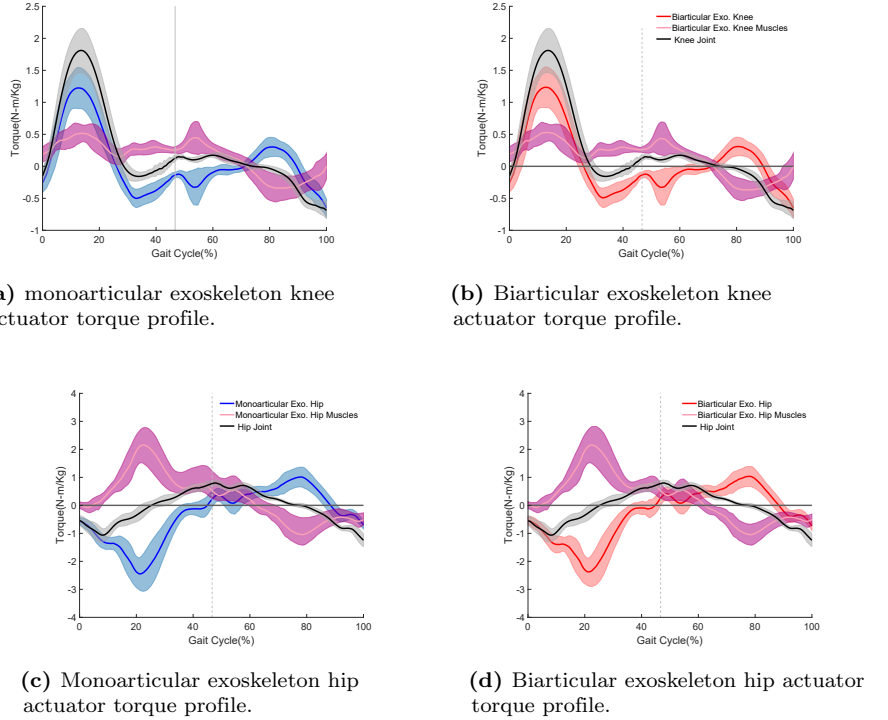


Fig 7. Monoarticular and biarticular exoskeletons hip and knee torque profiles compared to net joint moment and muscles generated moment.

from dynamics of the devices where monoarticular device's hip actuator should not only assist the assigned joint but also compensate the knee actuator's reaction force. This subject, as well as the assistive devices and muscles, generated moment profiles opposing will be studied in next sections.

It is worth mentioning that due to knee actuator assignment in biarticular and monoarticular exoskeletons, their torque profiles were not in the same reference frame. In order to transform the biarticular exoskeleton in the knee's generalized frame which joint moment and monoarticular torque were represented, we subtract the total knee muscles generated moment and knee reserve actuator from the net joint moment which results in the biarticular exoskeletons' knee actuator in the knee joint generalized frame:

$$\tau_{Bi.}^{F/T} = \tau_{Joint Moment}^{F/T} - \tau_{Muscles Moment}^{F/T} - \tau_{Reserve}^{F/T} \quad (21)$$

where T and F represent tibia and femur bodies respectively and all joint, muscle ,and reserve moment were calculated for knee joint. This method for transforming the torque to generalized frame was tested on monoarticular exoskeletons' actuators and Due to the same reference frame, the CMC reported and calculated torque were the same.

Similar to torque profiles, power profiles are also reaching their peak amount during the stance phase, and in most of the cases, they have a substantially different profile than the net joint power. Among the exoskeletons assisting specific joint, hip exoskeleton requires high positive power, especially during the mid-stance phase. Monoarticular knee exoskeleton at the initial phase of the gait, demonstrates remarkably high negative power which gives considerable potential for energy regeneration (Table 3) and then during the mid-stance and initial swing phases it required two high positive mechanical power; however, unlike the monoarticular knee,

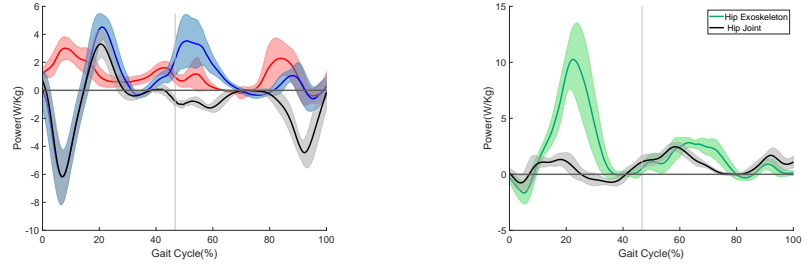


Fig 8. Assistive devices assisting single joint power and speed profiles compared to joints power and speed.

biarticular knee device performed mostly positive mechanical work with lower peak and mean power consumptions. This economic profile of biarticular knee device makes it highly efficient than monoarticular exoskeleton experiencing high variations in the power profile even with complete regeneration where all negative work can be restored to the battery. For the main configurations of the exoskeletons, monoarticular and biarticular has very similar power profiles in hip actuators but in the knee actuators, while they had two closely matching torque profiles, the power consumption of biarticular is remarkably economical than monoarticular device (Table 3) which is result of actuator's considerably lower velocity as shown in figure 9(d); velocity difference between mono. and biarticular knee actuators is due to the kinematics between them:

$$\omega_{femur}^{\text{femur}} = \omega_{torso}^{\text{tibia}} - \omega_{torso}^{\text{femur}} \quad (22)$$

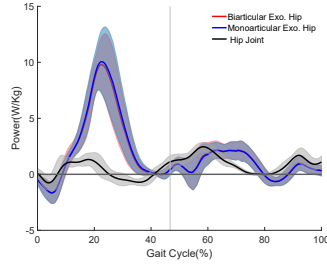
Moreover, same as the single joint exoskeletons, the peak power required during the stance phases of the gait cycle in both actuators of the exoskeletons where hip actuators and monoarticular knee have resemblant profiles with relevant single joint assistive devices with lower peak and mean positive power (Table 3). Biarticular knee, however, has a different profile than its assistive device profile where it has considerably more energy to be regenerated with a lower positive peak and mean power (Table 3).

Device Effect on Subjects Muscles

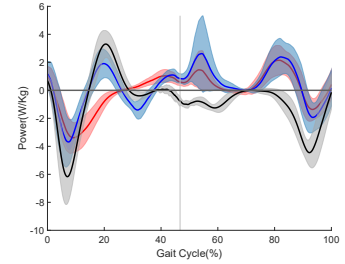
Adding an actuator to optimizer would affect the optimization result, and optimizer can find a more economical set of actuation to track the kinematics; therefore, assistive devices affect the subjects muscular activation which is the output of optimizer in CMC algorithm. This effect would not necessarily decrease all muscles activity, and it can be more economical to increase specific muscles activities during some phases of gait to track the kinematics with lower cost (i.e. metabolic power consumption).

Monoarticular knee assistive device dramatically decrease the vasti muscles (i.e. Vastus intermedius, Vastus lateralis, Vastus medialis) and Biceps femoris short head activations which are the knee extensor group of muscles and knee flexor muscle respectively. Rectus femoris activation is increased during the early swing, which is occurred because the hip flexion required moment production by rectus femoris is more economical [2, 93], and it can replace iliopsoas muscles providing moment. This behavior of optimizer explains why the actuator and muscles moment are opposing each other in some phases of the gait cycle and why it is selected by optimizer.

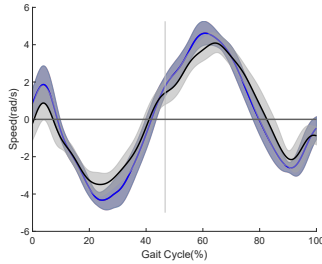
Hip muscles also affected by the hip bilateral exoskeleton, and the primary effect was observed in the rectus femoris where its activity increased considerably during stance



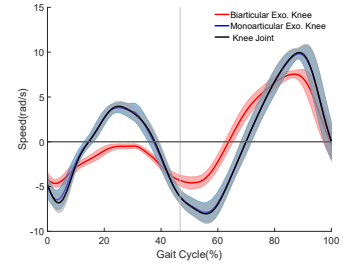
(a) Mono and Biarticular exoskeletons hip actuators power profiles



(b) Mono and Biarticular exoskeletons knee actuators power profiles



(c) Mono and Biarticular exoskeletons hip actuators speed profiles



(d) Mono and Biarticular exoskeletons knee actuators speed profiles

Fig 9. Monoarticular and biarticular devices power and speed profiles compared to joints power and speed.

phase enabling the vasti muscles activity to be decreased during stance phase. Hip exoskeleton increased the iliopsoas muscles, as the main muscles in providing hip flexion moment, activity is also increased during the mid-stance phase and then considerably decreased in the rest of the gait cycle. Finally, Gluteus maximus, minimus, and medius muscles activity as a hip extensor muscles were decreased by the hip exoskeleton during stance phase. These results for monoarticular knee and hip exoskeletons support the result of Uchida et al. [2], and we would refer readers for more detailed analysis of muscles to their paper.

Biarticular knee exoskeleton has an utterly different effect on the assisted subjects muscle activities than monoarticular knee exoskeleton. This device does not dramatically decrease any muscles activity, which is not surprising due to its low assistance level. Biarticular knee device increased all knee extensor muscles activities (i.e. vasti and rectus femoris muscles) during stance phase, and rectus femoris increase was remarkable during the stance phase and similar to the hip device; this behavior of muscles in the knee during the stance phase explains the actuator and muscles moments contraction. Biarticular knee device affects Biceps femoris long and short head, and it decreases their overall activity, especially during the stance phase. Semitendinosus as a knee flexor muscle is also affected by biarticular knee device considerably during stance phase. Biarticular knee exoskeleton also profoundly affect most of the hip muscles unlike the monoarticular one and this effect is more evident in hip extensor muscles where it decreased Gluteus maximus, minimus, and medius muscles activity as a hip extensor muscles.

Biarticular and Monoarticular exoskeletons assisting hip and knee have a quite similar effect on the subjects muscular activities which could be inferred from their

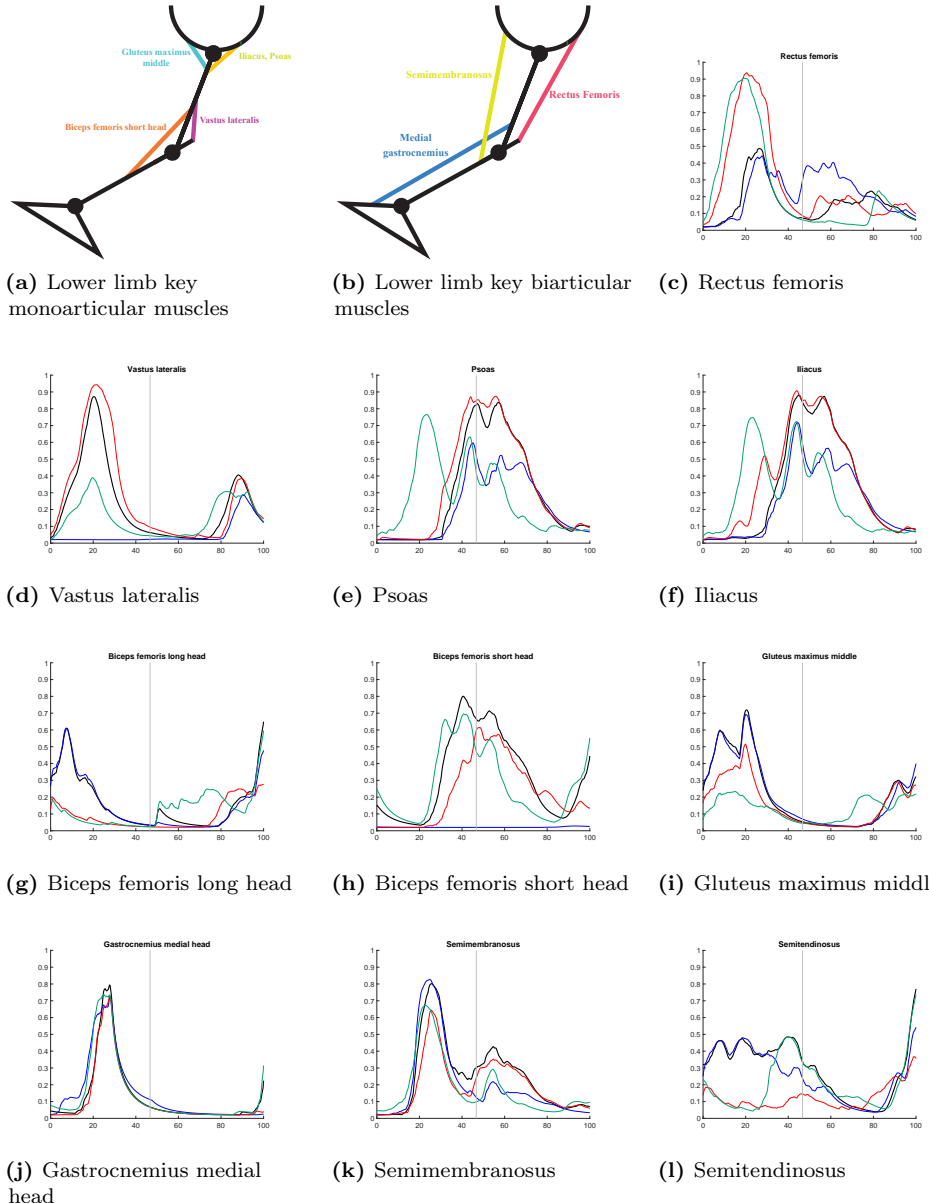


Fig 10. Single joint assistive devices effect on the subjects muscles activation. Red, green and blue profiles represent biarticular knee, hip ,and monoarticular knee exoskeletons effect on the specific muscle.

torque profiles. Vasti muscles activity dramatically decreased, and rectus femoris activity increased during stance phase to take advantage of high force production capability of it to provide the required moment more economically similar to hip and monoarticular knee exoskeletons; iliopsoas muscles also has activity increase in stance phase, and then their activity has notable reduction; these muscles activity can easily explain the muscles and assistive actuators behavior. Biceps femoris long and short head has dramatic reduction which was not observed on assisting knee with biarticular knee device. Gastrocnemius medial head has a negligible reduction in the late swing phase and during its peak; the reason for the low effect of the exoskeletons on this

muscle is its central role in providing the ankle's moment. Finally, Gluteus maximus, minimus, and medius muscles activity as a hip extensor muscles were decreased by both exoskeletons. We would refer the reader to supplementary material for devices effect on all of the muscles activation in all five configurations of the exoskeleton.

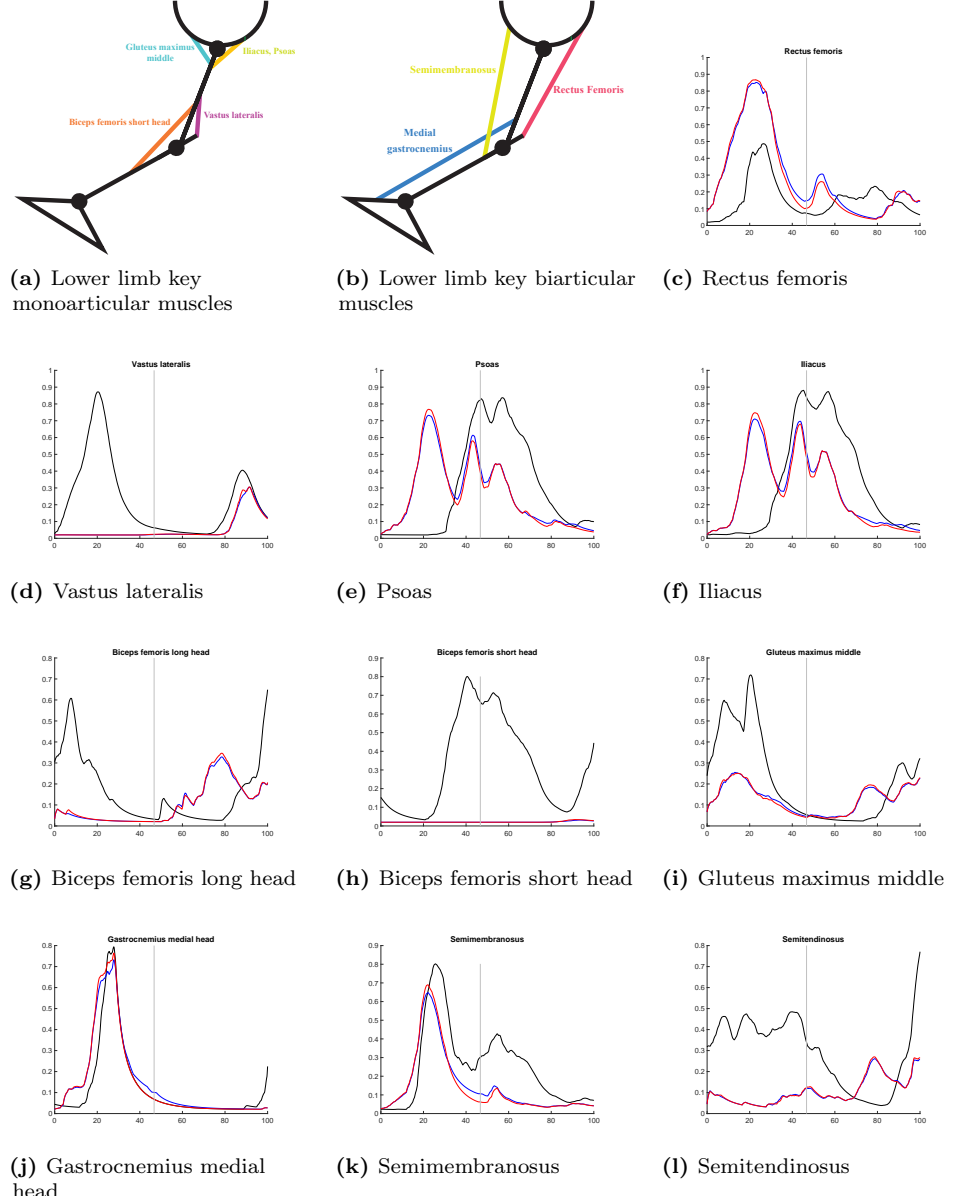


Fig 11. Monoarticular and Biarticular hip and knee bilateral exoskeletons effect on the subjects muscles activation. Red and blue profiles represent biarticular and monoarticular exoskeletons effect on the specific muscle.

Ideal Exoskeletons Result in Feasible Energy Region

To have more realistic results for the exoskeletons, we derived Pareto-front curves for monoarticular and biarticular which, as stated earlier, is not promised to be the global

optima for each subject but it enables to have a fair comparison between two configurations and also provide a broad view about average performance of the devices throughout the chosen cost functions. figure 12 shows the average trade-off between

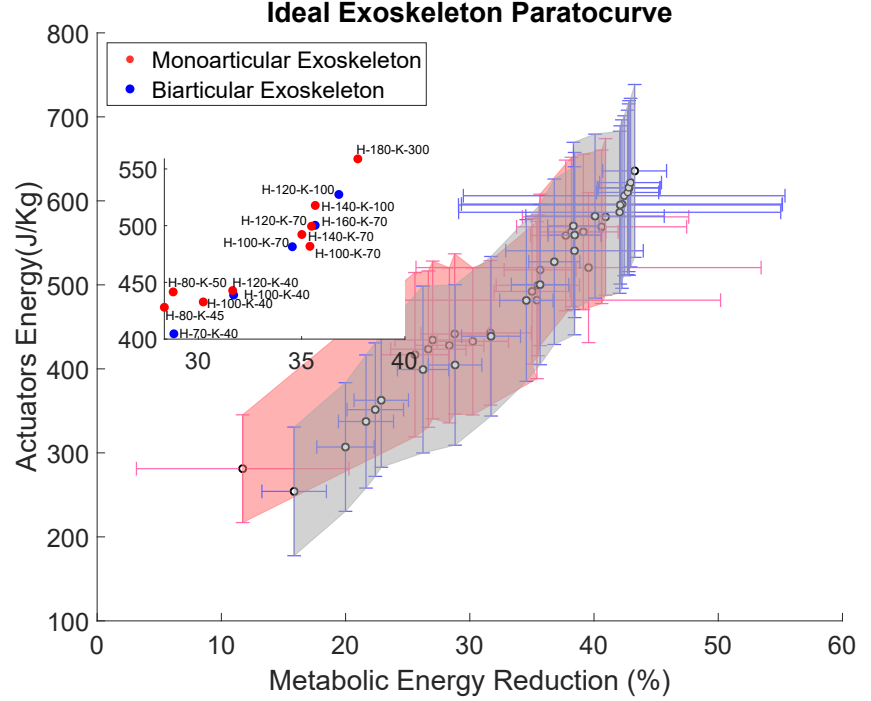


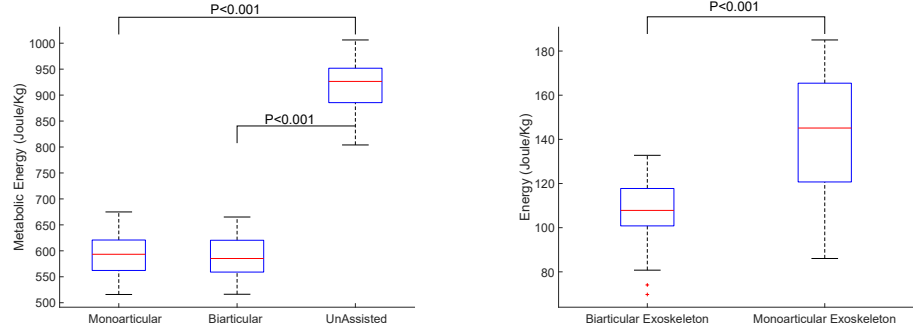
Fig 12. Monoarticular and Biarticulator hip and knee exoskeletons Pareto-front.

assistive actuators energy consumption and exoskeletons effect on metabolic cost reduction. Any point on these curves can be chosen as an average optima points based on the secondary criteria. There were some large deviations in the energy axis which were due to presence of some outlier data where we reduced their weight in standard deviation calculations, but the mean is calculated without excluding them; however, in higher weights, where metabolic cost reduction and energy consumption are quite high, even though we did not observe outliers but between the subject variations were high in this region which is due to high between the subject variation of hip actuators in both monoarticular and biarticulator assistive devices which also already observed by Uchida et al. [2] in their simulations.

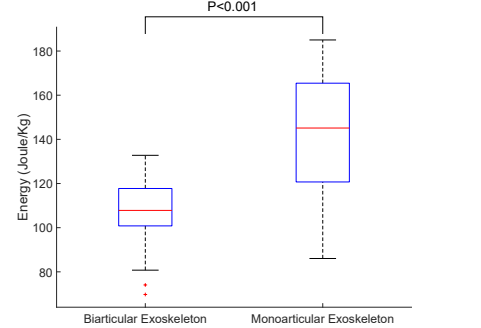
Our aim was to compare these two exoskeletons during lower energy consumption levels with two different weight to study the effect of selected weight and lower energy consumption on their performance. To this end, we chose biarticulator exoskeleton with hip and knee weights (Optimal Force) 160 and 120 (N-m) respectively and monoarticular with hip and knee optimal force 70 and 70 (N-m) where it is shown on the figure 12. As it can be inferred from the Pareto front curves, these two points have very similar performance in terms of the metabolic energy reduction and actuators energy consumption making possible to have a fair comparison between biarticulator and monoarticular exoskeletons.

Device Performance, Torque and Power

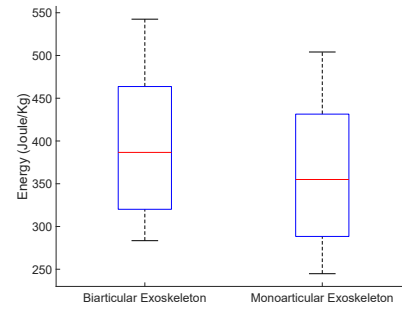
Both devices reduced the subjects metabolic cost considerably where biarticulator and monoarticular devices cause $35.48 \pm 3.64\%$ and $35.66 \pm 3.17\%$ reduction on the metabolic



(a) Assisted subjects lower extremity muscles average metabolic energy consumption.



(b) Ideal biarticular and monoarticular exoskeletons knee actuators energy consumption



(c) Ideal biarticular and monoarticular exoskeletons hip actuators energy consumption

Fig 13. Ideal exoskeletons with lower energy consumption effect on the 7 running subjects metabolic and actuators energy expenditures.

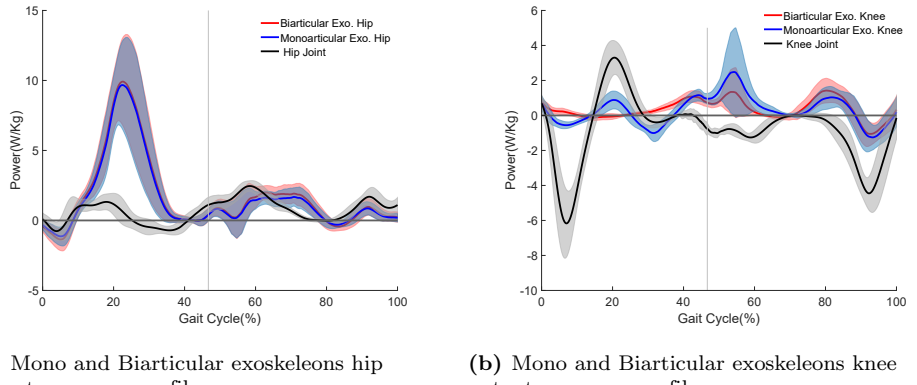
power consumption of 7 subjects running in 2 m/s. To achieve this metabolic cost reduction, biarticular and monoarticular devices hip actuators consumed 1.86 ± 0.44 and 1.73 ± 0.45 (W/Kg) and the knee actuators consumed 0.44 ± 0.07 and 0.52 ± 0.13 (W/Kg) average positive power (Table 4). Although both devices provide very close assistance to the subjects, biarticular power consumption is economical than monoarticular thanks to biarticular knee configuration of the device. However, unlike the devices with maximum performance, the biarticular hip actuator has higher energy consumption (Table 4).

Figure 14 represents the power profiles of the biarticular and monoarticular assistive devices. As it can be seen in figure 14 (a), the biarticular hip actuator has higher power consumption than monoarticular one during the stance phase and after toe-off. Another remarkable change is biarticular knee actuator power profile (Fig. 14 (a)) where it consumed power during the early stance phase, which is unlike to exoskeleton with maximum performance. Furthermore, it can be easily inferred that energy regeneration will not be effective in this assistance level since all actuators are performing an insignificant amount of negative mechanical work. Torque profiles of the hip actuators are similar to the assistive devices with maximum performance; however, knee profiles had considerable changes where they do not oppose with muscles generated moment during the stance phases, and their magnitude are considerably reduced.

It is noteworthy that the biarticular knee actuator's frame has been transformed using transformation on Eq 21; due to this operation, some numerical errors appeared

Table 4. Ideal exoskeletons with feasible energy consumption power, energy consumption, metabolic power, and ratios.

Device	Actuator	Mean Metabolic Power (W/kg)	Peak Positive Power (W/kg)	Mean Positive power (W/kg)	Mean Energy Power (W/kg)	Metabolic to Peak Power Ratio	Metabolic to Mean Power Ratio
Monoarticular Hip+Knee	Total	5.87 ± 0.40					
	Hip Actuator		10.33 ± 2.76	1.73 ± 0.45	185.99±47.39	0.61±0.28	3.62±1.01
Biarticular Hip+Knee	Knee Actuator		2.97 ± 0.94	0.52± 0.13	75.46±10.12	2.77±0.01	12.57±0.04
	Total	5.88± 0.45					
	Hip Actuator		10.56 ± 2.64	1.86 ± 0.44	201.90±47.70	0.59±0.27	3.32±0.83
	Knee Actuator		2.17 ± 0.43	0.44 ±0.07	55.12±15.63	3.12±0.01	13.72±0.03



(a) Mono and Biarticular exoskeleons hip actuators power profiles **(b)** Mono and Biarticular exoskeleons knee actuators power profiles

Fig 14. Devices power and speed profiles compared to joints power and speed.

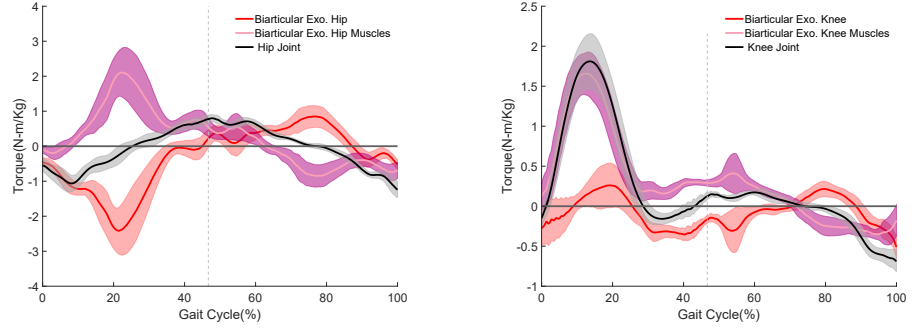
as a small variation on the biarticular knee profile, and higher standard deviation appeared which is more evident during stance phase.

Device Effect on Subject Muscles

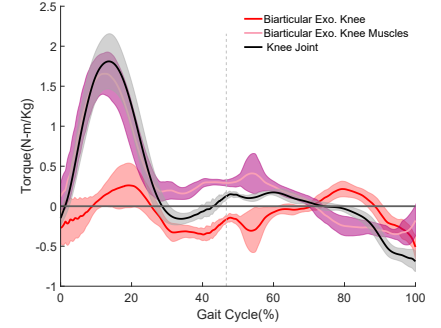
Most of the muscles are affected by assistive devices similar to the devices with maximum performance, however, unlike the previous case, no muscle was almost disabled which is not surprising due to the assistance level and the actuators torque profiles.

One of the main changes is that we cannot observe any dramatic reduction of muscular activation such as Biceps femoris short head (Fig. 16(h)) which was almost entirely deactivated by the optimizer when devices were with their maximum performance, and all muscles are considerably involved by optimizer to provide necessary torque for tracking the joints kinematics. Vasti muscles (Fig. 16(d)) were also deactivated due to presence of assistive actuators with negligible cost function and optimizer were finding assistive actuators more economical to use than the muscles; however, these devices have higher cost functions making the optimizer to consider trade-off between the vasti muscles and the actuators where it result in more activity and metabolic cost reduction on the subjects. It can be easily inferred from the knee extensor muscles activation that monoarticular device is more effective than biarticular on assisting the knee.

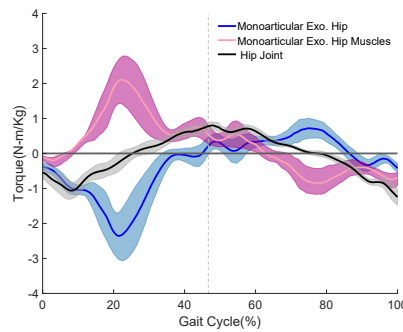
Rectus femoris (Fig. 16(c)) activation was increased similar to the previous case with the difference that monoarticular made it less active than the biarticular device; another notable change can be seen in Biceps femoris long head (Fig. 16(g)) and Semitendinosus(Fig. 16(l)) muscles where they were providing negligible moment during the stance phases in previous assistance scenario, however, they got activated during the



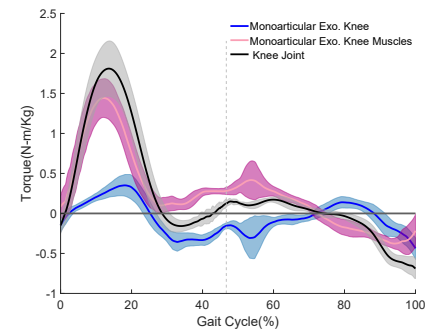
(a) Mono and Biarticular exoskeleons hip actuators power profiles



(b) Mono and Biarticular exoskeleons knee actuators power profiles



(c) Mono and Biarticular exoskeleons hip actuators power profiles



(d) Mono and Biarticular exoskeleons knee actuators power profiles

Fig 15. Devices power and speed profiles compared to joints power and speed.

stance phases in the feasible energy region. Most of the other muscles activation profile has minor changes like Gastrocnemius medial head, Gluteus maximus middle muscles.

Although most of the muscles with a central role in generating necessary muscles moment such as rectus femoris, iliopsoas are highly activated during stance phase, the total metabolic power of the assisted subjects was reduced. There are three major reasons to explain this; First and foremost reason is that major portion of the metabolic cost is affected by remaining muscles, as shown in [2], which mostly experienced reduction in their activation; secondly, vasti and Gluteus maximus muscles constitute notable portion of metabolic power which experienced high activation reduction during stance phase which can compensate for the highly activated muscles metabolic cost. Another issue that needs to be highlighted is that while iliopsoas muscles were experiencing increase during mid-stance and terminal stance phases, their activation during next phases, which is a big fraction of the gait cycle, is considerably decreased. This reduction resulting in iliopsoas muscles metabolic cost reduction; similarly, rectus femoris activation is decreased in major part of swing phase which can result in marginal metabolic energy consumption reduction which is observed for the assistive device simulated by Uchida et al. [2].

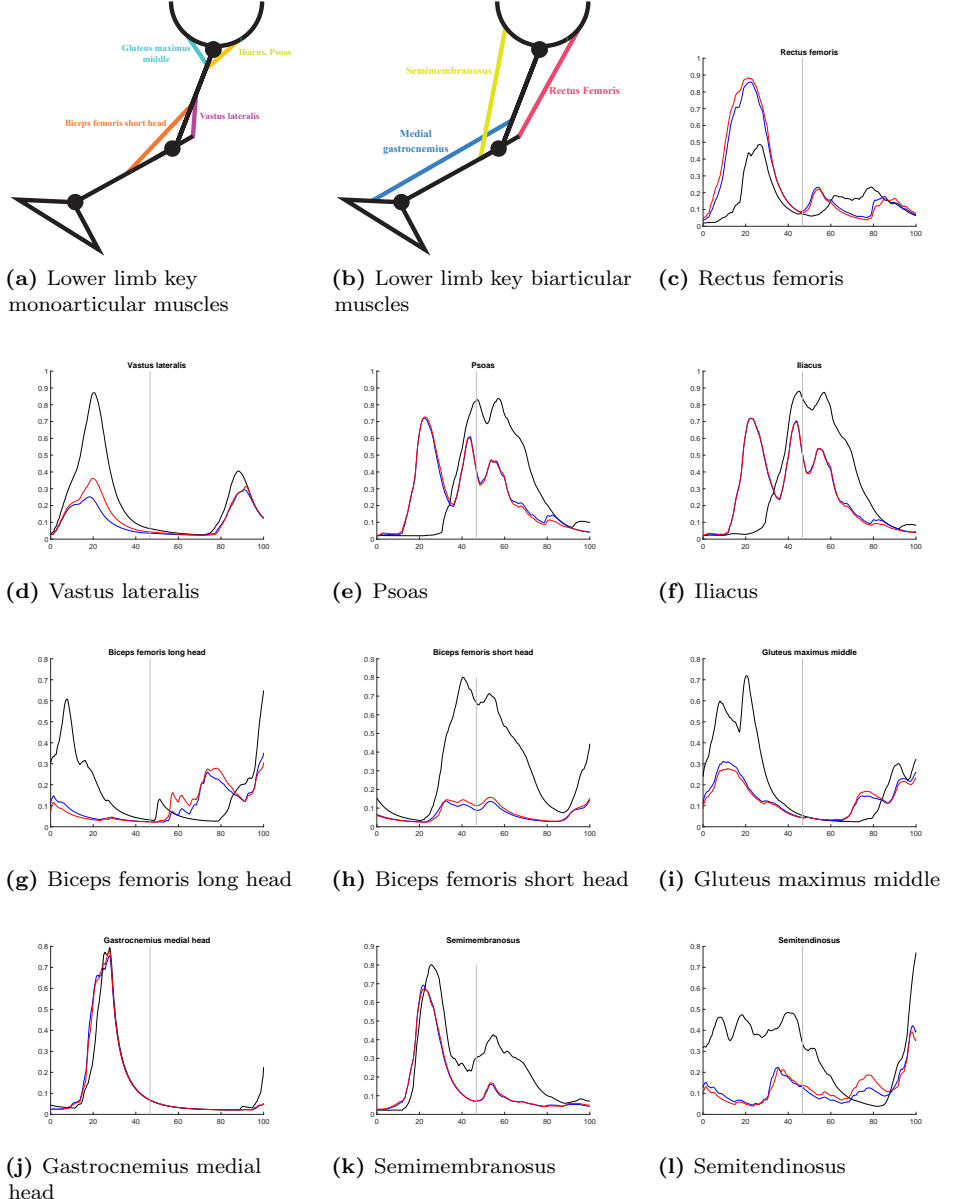


Fig 16. Monoarticular and Biarticular hip and knee bilaterals exoskeletons with feasible energy consumption effect on the subjects muscles activation. Red and blue profiles represent biarticular and monoarticular exoskeletons effect on the specific muscle.

Study Limitations

This simulation-based studying assistive device has some limitations that need to be considered for any interpretation of the results. One of the main limitations is kinematics and ground reaction forces for the assisted subjects; Although experimental studies reported that exoskeleton could make a minor [42, 84, 90, 116–118] and significant [85, 119–121] changes on assisted subjects kinematics and joint moment, our simulator's algorithm (CMC) is not capturing these changes and it is assumed that unassisted and assisted subjects have the same kinematics, ground reaction force, and

joint moment, nonetheless, it is reported that metabolic cost may not substantially be affected by kinematics changes [122]. This limitation recently has been addressed by employing predictive simulations which can capture the changes in the kinematics and dynamics of the assisted subjects.

Secondly, as it is earlier stated, assistive devices that we modeled was assumed massless without any actuator and link mass and inertia; yet, in practice, exoskeleton actuation modules mass and their reflected inertia on the links are large and one of the main challenges on mechanical design of the exoskeletons and also it is proven that adding mass the lower limbs can considerably change metabolic cost of the subjects. The exoskeletons attachment on the body is also one of the central performance limiting factors of the assistive devices [123] which is not modeled in ideal exoskeletons.

Another significant limitation of this study is limitations on musculoskeletal modeling. There are some influential restrictions on muscles modeling that affect the assistive devices simulations results. One of these restraints is extortionate passive force generated by the muscles [92], that can result in extortionate muscular activities which observed by similar work [93] when they were comparing simulation and experimental muscular activities. Another critical issue in Hill-type muscles modeling is that it does not take into account the muscle fatigue, which is an effective factor in muscle recruitment strategies [92]. Rectus femoris, which is more vulnerable to fatigue due to its fibers properties [124] was experiencing extreme activations in all of the assistance scenarios, which in practice may cause subjects muscles fatigue [125]. Tendon modeling, constant force enhancement, short-range muscle stiffness and some other factors [92] are limiting aspects of the muscles that affect the musculoskeletal models and the simulations results which need to be considered for any interpretation of this study's results.

Conducting Pareto optimization is introducing another limitation on this study because we used average Pareto front where a subject's optima points were searched, and its Pareto front weights were repeated for all of the subjects. While this method resulted in a very similar Pareto with standard deviation, we cannot claim anything about its global optimality. The reason for this method was simulation time, and extensive range of weight, need to be searched, were not feasible to conduct on seven different subjects with three trials and feasibility of this exhaustive search leads to highly discretized and a single subject search. Therefore, readers should take this search's limitation as well as other study's restraints into consideration for any interpretation of the results.

We also would refer the readers to similar papers [2,93], where they also discussed their studies limitation, which is similar in most of the aspects. Moreover, [92] provides comprehensive information about all aspects of the OpenSim simulations and propose some recommendation for any interpretation and validation of the simulations that can be beneficial to have an accurate interpretation of our results.

Conclusions and Future Work

In this study, we investigate how introducing biarticular configuration on assistive devices can affect the exoskeletons efficiency, assisted subjects muscles activity and their energy expenditure when running with 2 m/s speed by using musculoskeletal simulations. We introduced new configurations of the exoskeleton for knee and knee + Hip which can provide assistance with considerably higher efficiency in comparison with monoarticular configuration which can lead the exoskeleton design to get more effective assistive devices.

Thanks to musculoskeletal simulations we are given insight into how energy was consumed during a gait cycle and which phase of the gait exoskeletons require more

energy and where we can harvest energy to charge the battery on untethered exoskeletons and also we could show that in lower energy consumptions, actuators power profile would not be effective for regeneration. This stage of the study can further help the designer to decide about the battery and its regeneration design. Taking advantage of the multi-criteria optimization concept to acquire the average Pareto front for each configuration enabled us to address how to compare different configurations of assistive devices while in different energy consumptions areas. This would help researchers and designers to simulate exoskeletons with their specifications such as energy consumption and torque requirement.

As future work, we will take into account the monoarticular and biarticular exoskeletons inertial properties which have been designed in our group to study our assistive devices effect on the running subjects energy expenditure, muscles activity and how adding inertia can affect the torque and power profiles. As it is discussed in the limitations of the study, global or dynamic optimization needs to be replaced by static optimization during the simulations which is called predictive simulation [96, 100] which will capture any ground reaction force, joint moment and kinematics changes and it should be one of the main future works for studying the exoskeletons effect on subjects suggested by the relevant researches [2, 93] as well. SCONE [126] is open-source software designed for performing predictive simulations of biological motion which can be used to study the assistive devices.

Simulations based on the Pareto front had limitations highlighted in the previous section, which should be addressed in future work. Infeasibility of the search and big discretization can be addressed by using normal boundary intersection method [110] which is designed for this purpose to resolve these issues on computationally heavy problems resulting in more accurate with lower discretization issue Pareto front for the subjects.

Simulations outcomes are beneficial as a prior information to assist the subjects, and they can be used on human in the loop optimization [127] as a prior profile to start optimization with the simulations torque profiles which may result in less optimization time by increasing convergence rate of the optimization; we will establish experimental setup and validate our simulations with inertial properties using experimental outcomes, then, human in the loop optimization may also examined using the simulations profiles in the next phases of this research.

Supporting information

S1 Fig. Bold the title sentence. Add descriptive text after the title of the item (optional).

S2 Fig. Lorem ipsum. Maecenas convallis mauris sit amet sem ultrices gravida. Etiam eget sapien nibh. Sed ac ipsum eget enim egestas ullamcorper nec euismod ligula. Curabitur fringilla pulvinar lectus consectetur pellentesque.

S1 File. Lorem ipsum. Maecenas convallis mauris sit amet sem ultrices gravida. Etiam eget sapien nibh. Sed ac ipsum eget enim egestas ullamcorper nec euismod ligula. Curabitur fringilla pulvinar lectus consectetur pellentesque.

S1 Video. Lorem ipsum. Maecenas convallis mauris sit amet sem ultrices gravida. Etiam eget sapien nibh. Sed ac ipsum eget enim egestas ullamcorper nec euismod ligula. Curabitur fringilla pulvinar lectus consectetur pellentesque.

S1 Appendix. Lorem ipsum. Maecenas convallis mauris sit amet sem ultrices gravida. Etiam eget sapien nibh. Sed ac ipsum eget enim egestas ullamcorper nec euismod ligula. Curabitur fringilla pulvinar lectus consectetur pellentesque.

S1 Table. Lorem ipsum. Maecenas convallis mauris sit amet sem ultrices gravida. Etiam eget sapien nibh. Sed ac ipsum eget enim egestas ullamcorper nec euismod ligula. Curabitur fringilla pulvinar lectus consectetur pellentesque.

Acknowledgments

We sincerely thank OpenSim community for their help during this research; especially, we thank Thomas Uchida, Dimitar Stanev, and James Dunne for answering most of our questions about the OpenSim.

References

1. Rodman PS, McHenry HM. Bioenergetics and the origin of hominid bipedalism. *American Journal of Physical Anthropology*. 1980;52(1):103–106. doi:10.1002/ajpa.1330520113.
2. Uchida TK, Seth A, Pouya S, Dembia CL, Hicks JL, Delp SL. Simulating Ideal Assistive Devices to Reduce the Metabolic Cost of Running. *PLOS ONE*. 2016;11(9):1–19. doi:10.1371/journal.pone.0163417.
3. Carrier DR, Kapoor AK, Kimura T, Nickels MK, Satwanti, Scott EC, et al. The Energetic Paradox of Human Running and Hominid Evolution [and Comments and Reply]. *Current Anthropology*. 1984;25(4):483–495.
4. Fedak M, Pinshow B, Schmidt-Nielsen K. Energy cost of bipedal running. *American Journal of Physiology-Legacy Content*. 1974;227(5):1038–1044. doi:10.1152/ajplegacy.1974.227.5.1038.
5. Schalock RL. The concept of quality of life: what we know and do not know. *Journal of Intellectual Disability Research*;48(3):203–216. doi:10.1111/j.1365-2788.2003.00558.x.
6. Aoyagi Y, Shephard RJ. Aging and Muscle Function. *Sports Medicine*. 1992;14(6):376–396. doi:10.2165/00007256-199214060-00005.
7. Doherty TJ, Vandervoort AA, Brown WF. Effects of Ageing on the Motor Unit: A Brief Review. *Canadian Journal of Applied Physiology*. 1993;18(4):331–358. doi:10.1139/h93-029.
8. Brooks SV, Faulkner JA. 1994, Skeletal Muscle Weakness in Old Age: Underlying Mechanisms. *Sci Sports Exercise*;26:432–439.
9. Thelen DG, Schultz AB, Alexander NB, Ashton-Miller JA. Effects of Age on Rapid Ankle Torque Development. *The Journals of Gerontology: Series A*. 1996;51A(5):M226–M232. doi:10.1093/gerona/51A.5.M226.
10. Porter MM, Vandervoort AA, Kramer JF. Eccentric Peak Torque of the Plantar and Dorsiflexors Is Maintained in Older Women. *The Journals of Gerontology: Series A*. 1997;52A(2):B125–B131. doi:10.1093/gerona/52A.2.B125.

11. Vandervoort AA, McComas AJ. Contractile changes in opposing muscles of the human ankle joint with aging. *Journal of Applied Physiology*. 1986;61(1):361–367. doi:10.1152/jappl.1986.61.1.361.
12. Vandervoort AA, Chesworth BM, Cunningham DA, Paterson DH, Rechnitzer PA, Koval JJ. Age and Sex Effects on Mobility of the Human Ankle. *Journal of Gerontology*. 1992;47(1):M17–M21. doi:10.1093/geronj/47.1.M17.
13. Gajdosik RL, Vander Linden DW, Williams AK. Influence of age on concentric isokinetic torque and passive extensibility variables of the calf muscles of women. *European Journal of Applied Physiology and Occupational Physiology*. 1996;74(3):279–286. doi:10.1007/BF00377451.
14. DG T. Adjustment of Muscle Mechanics Model Parameters to Simulate Dynamic Contractions in Older Adults. doi: ASME; 2003.
15. Brown-Triolo DL, Roach MJ, Nelson KA, Triolo RJ. Consumer perspectives on mobility: implications for neuroprostheses design. *Journal of rehabilitation research and development*. 2002;39 6:659–69.
16. Farris DJ, Hampton A, Lewek MD, Sawicki GS. Revisiting the mechanics and energetics of walking in individuals with chronic hemiparesis following stroke: from individual limbs to lower limb joints. *Journal of NeuroEngineering and Rehabilitation*. 2015;12(1):24. doi:10.1186/s12984-015-0012-x.
17. Olney SJ, Richards C. Hemiparetic gait following stroke. Part I: Characteristics. *Gait & Posture*. 1996;4(2):136 – 148.
doi:[https://doi.org/10.1016/0966-6362\(96\)01063-6](https://doi.org/10.1016/0966-6362(96)01063-6).
18. Richards CL, Malouin F, Dean C. Gait in Stroke: Assessment and Rehabilitation. *Clinics in Geriatric Medicine*. 1999;15(4):833 – 856.
doi:[https://doi.org/10.1016/S0749-0690\(18\)30034-X](https://doi.org/10.1016/S0749-0690(18)30034-X).
19. Balasubramanian CK, Neptune RR, Kautz SA. Variability in spatiotemporal step characteristics and its relationship to walking performance post-stroke. *Gait & Posture*. 2009;29(3):408 – 414.
doi:<https://doi.org/10.1016/j.gaitpost.2008.10.061>.
20. Duncan PW, Sullivan KJ, Behrman AL, Azen SP, Wu SS, Nadeau SE, et al. Body-Weight-Supported Treadmill Rehabilitation after Stroke. *New England Journal of Medicine*. 2011;364(21):2026–2036. doi:10.1056/NEJMoa1010790.
21. Cruz TH, Lewek MD, Dhaher YY. Biomechanical impairments and gait adaptations post-stroke: Multi-factorial associations. *Journal of Biomechanics*. 2009;42(11):1673 – 1677. doi:<https://doi.org/10.1016/j.jbiomech.2009.04.015>.
22. Moriello C, Finch L, Mayo NE. Relationship between muscle strength and functional walking capacity among people with stroke. *Journal of rehabilitation research and development*. 2011;48 3:267–75.
23. Chen G, Patten C, Kothari DH, Zajac FE. Gait differences between individuals with post-stroke hemiparesis and non-disabled controls at matched speeds. *Gait & Posture*. 2005;22(1):51 – 56.
doi:<https://doi.org/10.1016/j.gaitpost.2004.06.009>.

24. Chen G, Patten C, Kothari DH, Zajac FE. Gait differences between individuals with post-stroke hemiparesis and non-disabled controls at matched speeds. *Gait & Posture*. 2005;22(1):51 – 56.
doi:<https://doi.org/10.1016/j.gaitpost.2004.06.009>.
25. Kubo K, Kanehisa H, Fukunaga T. Effects of resistance and stretching training programmes on the viscoelastic properties of human tendon structures in vivo. *The Journal of Physiology*;538(1):219–226. doi:10.1113/jphysiol.2001.012703.
26. Lichtwark GA, Wilson AM. Optimal muscle fascicle length and tendon stiffness for maximising gastrocnemius efficiency during human walking and running. *Journal of Theoretical Biology*. 2008;252(4):662 – 673.
doi:<https://doi.org/10.1016/j.jtbi.2008.01.018>.
27. Ruby BC, III GWL, Armstrong DW, Gaskill SE. Wildland firefighter load carriage: effects on transit time and physiological responses during simulated escape to safety zone. *International Journal of Wildland Fire*. 2003;12(1):111–116.
28. Knapik JJ, Reynolds KL, Harman E. Soldier Load Carriage: Historical, Physiological, Biomechanical, and Medical Aspects. *Military Medicine*. 2004;169(1):45–56. doi:10.7205/MILMED.169.1.45.
29. van Vuuren BJ, Becker PJ, van Heerden HJ, Zinzen E, Meeusen R. Lower back problems and occupational risk factors in a South African steel industry. *American Journal of Industrial Medicine*;47(5):451–457. doi:10.1002/ajim.20164.
30. Yagn N. Apparatus for facilitating walking, running, and jumping; 1890. Available from: <https://patents.google.com/patent/US420179A/en>.
31. Dollar AM, Herr H. Lower Extremity Exoskeletons and Active Orthoses: Challenges and State-of-the-Art. *IEEE Transactions on Robotics*. 2008;24(1):144–158. doi:10.1109/TRO.2008.915453.
32. Garcia E, Sater JM, Main J. Exoskeletons for Human Performance Augmentation (EHPA) : A Program Summary. *Journal of the Robotics Society of Japan*. 2002;20(8):822–826. doi:10.7210/jrsj.20.822.
33. Chu A, Kazerooni H, Zoss A. On the Biomimetic Design of the Berkeley Lower Extremity Exoskeleton (BLEEX). In: Proceedings of the 2005 IEEE International Conference on Robotics and Automation; 2005. p. 4345–4352.
34. Riener R, Lünenburger L, Maier IC, Colombo G, Dietz V. Locomotor Training in Subjects with Sensori-Motor Deficits: An Overview of the Robotic Gait Orthosis Lokomat. *Journal of Healthcare Engineering*. 2010;1(2).
35. Zeilig G, Weingarten H, Zwecker M, Dudkiewicz I, Bloch A, Esquenazi A. Safety and tolerance of the ReWalk™ exoskeleton suit for ambulation by people with complete spinal cord injury: A pilot study. *The Journal of Spinal Cord Medicine*. 2012;35(2):96–101. doi:10.1179/2045772312Y.0000000003.
36. Young AJ, Ferris DP. State of the Art and Future Directions for Lower Limb Robotic Exoskeletons. *IEEE Transactions on Neural Systems and Rehabilitation Engineering*. 2017;25(2):171–182. doi:10.1109/TNSRE.2016.2521160.
37. Viteckova S, Kutilek P, Jirina M. Wearable lower limb robotics: A review. *Biocybernetics and Biomedical Engineering*. 2013;33(2):96 – 105.
doi:<https://doi.org/10.1016/j.bbe.2013.03.005>.

38. Yan T, Cempini M, Oddo CM, Vitiello N. Review of assistive strategies in powered lower-limb orthoses and exoskeletons. *Robotics and Autonomous Systems*. 2015;64:120 – 136. doi:<https://doi.org/10.1016/j.robot.2014.09.032>.
39. Huo W, Mohammed S, Moreno JC, Amirat Y. Lower Limb Wearable Robots for Assistance and Rehabilitation: A State of the Art. *IEEE Systems Journal*. 2016;10(3):1068–1081. doi:[10.1109/JSYST.2014.2351491](https://doi.org/10.1109/JSYST.2014.2351491).
40. Malcolm P, Derave W, Galle S, De Clercq D. A Simple Exoskeleton That Assists Plantarflexion Can Reduce the Metabolic Cost of Human Walking. *PLOS ONE*. 2013;8(2):1–7. doi:[10.1371/journal.pone.0056137](https://doi.org/10.1371/journal.pone.0056137).
41. Mooney LM, Rouse EJ, Herr HM. Autonomous exoskeleton reduces metabolic cost of human walking during load carriage. *Journal of NeuroEngineering and Rehabilitation*. 2014;11(1):80. doi:[10.1186/1743-0003-11-80](https://doi.org/10.1186/1743-0003-11-80).
42. Collins SH, Wiggin MB, Sawicki GS. Reducing the energy cost of human walking using an unpowered exoskeleton. *Nature*. 2015;522:212 EP –.
43. Awad LN, Bae J, O'Donnell K, De Rossi SMM, Hendron K, Sloot LH, et al. A soft robotic exosuit improves walking in patients after stroke. *Science Translational Medicine*. 2017;9(400). doi:[10.1126/scitranslmed.aai9084](https://doi.org/10.1126/scitranslmed.aai9084).
44. Shamaei K, Cenciarini M, Adams AA, Gregorczyk KN, Schiffman JM, Dollar AM. Biomechanical Effects of Stiffness in Parallel With the Knee Joint During Walking. *IEEE Transactions on Biomedical Engineering*. 2015;62(10):2389–2401. doi:[10.1109/TBME.2015.2428636](https://doi.org/10.1109/TBME.2015.2428636).
45. BROWNING RC, MODICA JR, KRAM R, GOSWAMI A. The Effects of Adding Mass to the Legs on the Energetics and Biomechanics of Walking. *Medicine & Science in Sports & Exercise*. 2007;39(3).
46. Nasiri R, Ahmadi A, Ahmadabadi MN. Reducing the Energy Cost of Human Running Using an Unpowered Exoskeleton. *IEEE Transactions on Neural Systems and Rehabilitation Engineering*. 2018;26(10):2026–2032. doi:[10.1109/TNSRE.2018.2872889](https://doi.org/10.1109/TNSRE.2018.2872889).
47. Ding Y, Galiana I, Asbeck AT, De Rossi SMM, Bae J, Santos TRT, et al. Biomechanical and Physiological Evaluation of Multi-Joint Assistance With Soft Exosuits. *IEEE Transactions on Neural Systems and Rehabilitation Engineering*. 2017;25(2):119–130. doi:[10.1109/TNSRE.2016.2523250](https://doi.org/10.1109/TNSRE.2016.2523250).
48. Rosendo A, Iida F. Energy efficient hopping with Hill-type muscle properties on segmented legs. *Bioinspiration & Biomimetics*. 2016;11(3):036002. doi:[10.1088/1748-3190/11/3/036002](https://doi.org/10.1088/1748-3190/11/3/036002).
49. WVD. Human-exoskeleton interaction. TU Delft; 2015. Available from: <https://doi.org/10.4233/uuid:8cf37c65-a48c-476e-8dcc-eb97c06c26d9>.
50. Buschmann T, Ewald A, von Twickel A, Büschges A. Controlling legs for locomotion—insights from robotics and neurobiology. *Bioinspiration & Biomimetics*. 2015;10(4):041001. doi:[10.1088/1748-3190/10/4/041001](https://doi.org/10.1088/1748-3190/10/4/041001).
51. Schenau GJVI. From rotation to translation: Constraints on multi-joint movements and the unique action of bi-articular muscles. *Human Movement Science*. 1989;8(4):301 – 337. doi:[https://doi.org/10.1016/0167-9457\(89\)90037-7](https://doi.org/10.1016/0167-9457(89)90037-7).

52. Jacobs R, Bobbert MF, van Ingen Schenau GJ. Mechanical output from individual muscles during explosive leg extensions: The role of biarticular muscles. *Journal of Biomechanics*. 1996;29(4):513 – 523. doi:[https://doi.org/10.1016/0021-9290\(95\)00067-4](https://doi.org/10.1016/0021-9290(95)00067-4).
53. Junius K, Moltedo M, Cherelle P, Rodriguez-Guerrero C, Vanderborght B, Lefebvre D. Biarticular elements as a contributor to energy efficiency: biomechanical review and application in bio-inspired robotics. *Bioinspiration & Biomimetics*. 2017;12(6):061001. doi:10.1088/1748-3190/aa806e.
54. Prilutsky BI, Zatsiorsky VM. Optimization-Based Models of Muscle Coordination. *Exercise and Sport Sciences Reviews*. 2002;30(1):32–38.
55. van Leeuwen J, Aerts P, Pandy MG. Simple and complex models for studying muscle function in walking. *Philosophical Transactions of the Royal Society of London Series B: Biological Sciences*. 2003;358(1437):1501–1509. doi:10.1098/rstb.2003.1338.
56. Anderson FC, Pandy MG. Dynamic Optimization of Human Walking. *Journal of Biomechanical Engineering*. 2001;123(5):381–390. doi:10.1115/1.1392310.
57. Schenau GJVI. On the Action of Bi-Articular Muscles, a Review. *Netherlands Journal of Zoology*. 1989;40(3).
58. Landin D, Thompson M, Reid M. Actions of Two Bi-Articular Muscles of the Lower Extremity: A Review. *Journal of Clinical Medicine Research*. 2016;8(7).
59. Voronov AV. The Roles of Monoarticular and Biarticular Muscles of the Lower Limbs in Terrestrial Locomotion. *Human Physiology*. 2004;30(4):476–484. doi:10.1023/B:HUMP.0000036345.33099.4f.
60. van Ingen Schenau GJ, Bobbert MF, van Soest AJ. In: Winters JM, Woo SLY, editors. *The Unique Action of Bi-Articular Muscles in Leg Extensions*. New York, NY: Springer New York; 1990. p. 639–652. Available from: https://doi.org/10.1007/978-1-4613-9030-5_41.
61. Elftman H. The function of muscles in locomotion. *Am J Physiol*. 1939;125. doi:10.1152/ajplegacy.1939.125.2.357.
62. Jacobs R, Bobbert MF, van Ingen Schenau GJ. Mechanical output from individual muscles during explosive leg extensions: The role of biarticular muscles. *Journal of Biomechanics*. 1996;29(4):513 – 523. doi:[https://doi.org/10.1016/0021-9290\(95\)00067-4](https://doi.org/10.1016/0021-9290(95)00067-4).
63. Prilutsky BI, Zatsiorsky VM. Tendon action of two-joint muscles: Transfer of mechanical energy between joints during jumping, landing, and running. *Journal of Biomechanics*. 1994;27(1):25 – 34. doi:[https://doi.org/10.1016/0021-9290\(94\)90029-9](https://doi.org/10.1016/0021-9290(94)90029-9).
64. Elftman H. THE WORK DONE BY MUSCLES IN RUNNING. *American Journal of Physiology-Legacy Content*. 1940;129(3):672–684. doi:10.1152/ajplegacy.1940.129.3.672.
65. Prilutsky BI, Petrova LN, Raitsin LM. Comparison of mechanical energy expenditure of joint moments and muscle forces during human locomotion. *Journal of Biomechanics*. 1996;29(4):405 – 415. doi:[https://doi.org/10.1016/0021-9290\(95\)00083-6](https://doi.org/10.1016/0021-9290(95)00083-6).

66. Wells RP. Mechanical energy costs of human movement: An approach to evaluating the transfer possibilities of two-joint muscles. *Journal of Biomechanics*. 1988;21(11):955 – 964.
doi:[https://doi.org/10.1016/0021-9290\(88\)90134-0](https://doi.org/10.1016/0021-9290(88)90134-0).
67. Cleland J. On the Actions of Muscles passing over more than One Joint. *Journal of anatomy and physiology*. 1867;1(1):85–93.
68. Fenn WO. The Mechanics of Muscular Contraction in Man. *Journal of Applied Physics*. 1938;9(3):165–177. doi:10.1063/1.1710406.
69. English C. Stiffness behaviour in two degree of freedom mechanisms. Carleton University,Ottawa, Ontario; 1999.
70. Hogan N. The mechanics of multi-joint posture and movement control. *Biological Cybernetics*. 1985;52(5):315–331. doi:10.1007/BF00355754.
71. Hogan N. Adaptive control of mechanical impedance by coactivation of antagonist muscles. *IEEE Transactions on Automatic Control*. 1984;29(8):681–690. doi:10.1109/TAC.1984.1103644.
72. Hogan N. In: Winters JM, Woo SLY, editors. *Mechanical Impedance of Single- and Multi-Articular Systems*. New York, NY: Springer New York; 1990. p. 149–164. Available from: https://doi.org/10.1007/978-1-4613-9030-5_9.
73. McIntyre J, Mussa-Ivaldi FA, Bizzi E. The control of stable postures in the multijoint arm. *Experimental Brain Research*. 1996;110(2):248–264.
doi:10.1007/BF00228556.
74. Iida F, Rummel J, Seyfarth A. Bipedal walking and running with spring-like biarticular muscles. *Journal of Biomechanics*. 2008;41(3):656 – 667.
doi:<https://doi.org/10.1016/j.jbiomech.2007.09.033>.
75. Sharbafi MA, Rode C, Kurowski S, Scholz D, Möckel R, Radkhah K, et al. A new biarticular actuator design facilitates control of leg function in BioBiped3. *Bioinspiration & Biomimetics*. 2016;11(4):046003.
doi:10.1088/1748-3190/11/4/046003.
76. Roozing W, Ren Z, Tsagarakis NG. Design of a Novel 3-DoF Leg with Series and Parallel Compliant Actuation for Energy Efficient Articulated Robots. In: 2018 IEEE International Conference on Robotics and Automation (ICRA); 2018. p. 1–8.
77. Höppner H, Wiedmeyer W, van der Smagt P. A new biarticular joint mechanism to extend stiffness ranges. In: 2014 IEEE International Conference on Robotics and Automation (ICRA); 2014. p. 3403–3410.
78. Dean JC, Kuo AD. Elastic coupling of limb joints enables faster bipedal walking. *Journal of The Royal Society Interface*. 2009;6(35):561–573.
doi:10.1098/rsif.2008.0415.
79. Eilenberg MF, Kuan JY, Herr H. Development and Evaluation of a Powered Artificial Gastrocnemius for Transtibial Amputee Gait. *Journal of Robotics*. 2018;2018:15.
80. Endo K, Swart E, Herr H. An artificial gastrocnemius for a transtibial prosthesis. In: 2009 Annual International Conference of the IEEE Engineering in Medicine and Biology Society; 2009. p. 5034–5037.

81. Eilenberg MF, Endo K, Herr H. Biomechanic and Energetic Effects of a Quasi-Passive Artificial Gastrocnemius on Transtibial Amputee Gait. *Journal of Robotics*. 2018;2018:12.
82. Flynn L, Geeroms J, Jimenez-Fabian R, Vanderborght B, Vitiello N, Lefever D. Ankle-knee prosthesis with active ankle and energy transfer: Development of the CYBERLEGS Alpha-Prosthesis. *Robotics and Autonomous Systems*. 2015;73:4 – 15. doi:<https://doi.org/10.1016/j.robot.2014.12.013>.
83. Eslamy M, Grimmer M, Seyfarth A. Adding passive biarticular spring to active mono-articular foot prosthesis: Effects on power and energy requirement. In: 2014 IEEE-RAS International Conference on Humanoid Robots; 2014. p. 677–684.
84. Panizzolo FA, Galiana I, Asbeck AT, Siviy C, Schmidt K, Holt KG, et al. A biologically-inspired multi-joint soft exosuit that can reduce the energy cost of loaded walking. *Journal of NeuroEngineering and Rehabilitation*. 2016;13(1):43. doi:10.1186/s12984-016-0150-9.
85. Quinlivan BT, Lee S, Malcolm P, Rossi DM, Grimmer M, Siviy C, et al. Assistance magnitude versus metabolic cost reductions for a tethered multiarticular soft exosuit. *Science Robotics*. 2017;2(2). doi:10.1126/scirobotics.aah4416.
86. Wiggin MB, Sawicki GS, Collins SH. An exoskeleton using controlled energy storage and release to aid ankle propulsion. In: 2011 IEEE International Conference on Rehabilitation Robotics; 2011. p. 1–5.
87. Xiong C, Zhou T, Zhou L, Wei T, Chen W. Multi-articular passive exoskeleton for reducing the metabolic cost during human walking. In: 2019 Wearable Robotics Association Conference (WearRAcon); 2019. p. 63–67.
88. Seth A, Hicks JL, Uchida TK, Habib A, Dembia CL, Dunne JJ, et al. OpenSim: Simulating musculoskeletal dynamics and neuromuscular control to study human and animal movement. *PLOS Computational Biology*. 2018;14(7):1–20. doi:10.1371/journal.pcbi.1006223.
89. Selinger J, O'Connor S, Wong J, Donelan JM. Humans Can Continuously Optimize Energetic Cost during Walking. *Current Biology*. 2015;25(18):2452 – 2456. doi:<https://doi.org/10.1016/j.cub.2015.08.016>.
90. Gordon KE, Ferris DP. Learning to walk with a robotic ankle exoskeleton. *Journal of Biomechanics*. 2007;40(12):2636 – 2644. doi:<https://doi.org/10.1016/j.jbiomech.2006.12.006>.
91. Delp SL, Anderson FC, Arnold AS, Loan P, Habib A, John CT, et al. OpenSim: Open-Source Software to Create and Analyze Dynamic Simulations of Movement. *IEEE Transactions on Biomedical Engineering*. 2007;54(11):1940–1950. doi:10.1109/TBME.2007.901024.
92. Hicks JL, Uchida TK, Seth A, Rajagopal A, Delp SL. Is My Model Good Enough?: Best Practices for Verification and Validation of Musculoskeletal Models and Simulations of Movement. *Journal of Biomechanical Engineering*. 2015;137(2):020905–020905–24. doi:10.1115/1.4029304.
93. Dembia CL, Silder A, Uchida TK, Hicks JL, Delp SL. Simulating ideal assistive devices to reduce the metabolic cost of walking with heavy loads. *PLOS ONE*. 2017;12(7):1–25. doi:10.1371/journal.pone.0180320.

94. Gordon DFN, Henderson G, Vijayakumar S. Effectively Quantifying the Performance of Lower-Limb Exoskeletons Over a Range of Walking Conditions. *Frontiers in Robotics and AI*. 2018;5:61. doi:10.3389/frobt.2018.00061.
95. Ong CF, Hicks JL, Delp SL. Simulation-Based Design for Wearable Robotic Systems: An Optimization Framework for Enhancing a Standing Long Jump. *IEEE Transactions on Biomedical Engineering*. 2016;63(5):894–903. doi:10.1109/TBME.2015.2463077.
96. Dorn TW, Wang JM, Hicks JL, Delp SL. Predictive Simulation Generates Human Adaptations during Loaded and Inclined Walking. *PLOS ONE*. 2015;10(4):1–16. doi:10.1371/journal.pone.0121407.
97. Nguyen VQ, Umberger BR, Sup FC. Predictive Simulation of Human Walking Augmented by a Powered Ankle Exoskeleton. In: 2019 IEEE 16th International Conference on Rehabilitation Robotics (ICORR); 2019. p. 53–58.
98. LaPrè AK, Umberger BR, Sup F. Simulation of a powered ankle prosthesis with dynamic joint alignment. In: 2014 36th Annual International Conference of the IEEE Engineering in Medicine and Biology Society; 2014. p. 1618–1621.
99. Zhao J, Berns K, de Souza Baptista R, Bó APL. Design of variable-damping control for prosthetic knee based on a simulated biped. In: 2013 IEEE 13th International Conference on Rehabilitation Robotics (ICORR); 2013. p. 1–6.
100. Handford ML, Srinivasan M. Robotic lower limb prosthesis design through simultaneous computer optimizations of human and prosthesis costs. *Scientific Reports*. 2016;6:19983 EP –.
101. Handford ML, Srinivasan M. Energy-Optimal Human Walking With Feedback-Controlled Robotic Prostheses: A Computational Study. *IEEE Transactions on Neural Systems and Rehabilitation Engineering*. 2018;26(9):1773–1782. doi:10.1109/TNSRE.2018.2858204.
102. Sreenivasa M, Millard M, Felis M, Mombaur K, Wolf SI. Optimal Control Based Stiffness Identification of an Ankle-Foot Orthosis Using a Predictive Walking Model. *Frontiers in Computational Neuroscience*. 2017;11:23. doi:10.3389/fncom.2017.00023.
103. Fey NP, Klute GK, Neptune RR. Optimization of Prosthetic Foot Stiffness to Reduce Metabolic Cost and Intact Knee Loading During Below-Knee Amputee Walking: A Theoretical Study. *Journal of Biomechanical Engineering*. 2012;134(11). doi:10.1115/1.4007824.
104. Rajagopal A, Dembia CL, DeMers MS, Delp DD, Hicks JL, Delp SL. Full-Body Musculoskeletal Model for Muscle-Driven Simulation of Human Gait. *IEEE Transactions on Biomedical Engineering*. 2016;63(10):2068–2079.
105. Thelen DG, Anderson FC, Delp SL. Generating dynamic simulations of movement using computed muscle control. *Journal of Biomechanics*. 2003;36(3):321 – 328. doi:[https://doi.org/10.1016/S0021-9290\(02\)00432-3](https://doi.org/10.1016/S0021-9290(02)00432-3).
106. UMBERGER BR, GERRITSEN KGM, MARTIN PE. A Model of Human Muscle Energy Expenditure. *Computer Methods in Biomechanics and Biomedical Engineering*. 2003;6(2):99–111. doi:10.1080/1025584031000091678.

107. Uchida TK, Hicks JL, Dembia CL, Delp SL. Stretching Your Energetic Budget: How Tendon Compliance Affects the Metabolic Cost of Running. *PLOS ONE*. 2016;11(3):1–19. doi:10.1371/journal.pone.0150378.
108. Marler R, Arora JS. Survey of multi-objective optimization methods for engineering. *Structural and Multidisciplinary Optimization*. 2004;26:369–395.
109. Unal R, Kiziltas G, Patoglu V. Multi-criteria Design Optimization of Parallel Robots. In: 2008 IEEE Conference on Robotics, Automation and Mechatronics; 2008. p. 112–118.
110. Das I, Dennis J. Normal-Boundary Intersection: A New Method for Generating the Pareto Surface in Nonlinear Multicriteria Optimization Problems. *SIAM Journal on Optimization*. 1998;8(3):631–657. doi:10.1137/S1052623496307510.
111. Browning RC, Modica JR, Kram R, Goswami A. The effects of adding mass to the legs on the energetics and biomechanics of walking. *Medicine & Science in Sports & Exercise*. 2007;39(3):515–525.
112. Royer TD, Martin PE. Manipulations of leg mass and moment of inertia: effects on energy cost of walking. *Medicine & Science in Sports & Exercise*. 2005;37(4):649–656.
113. Soule RG, Goldman RF. Energy cost of loads carried on the head, hands, or feet. *Journal of Applied Physiology*. 1969;27(5):687–690. doi:10.1152/jappl.1969.27.5.687.
114. Huang TwP, Kuo AD. Mechanics and energetics of load carriage during human walking. *Journal of Experimental Biology*. 2014;217(4):605–613. doi:10.1242/jeb.091587.
115. Silder A, Delp SL, Besier T. Men and women adopt similar walking mechanics and muscle activation patterns during load carriage. *Journal of Biomechanics*. 2013;46(14):2522–2528. doi:10.1016/j.jbiomech.2013.06.020.
116. Jackson RW, Collins SH. An experimental comparison of the relative benefits of work and torque assistance in ankle exoskeletons. *Journal of Applied Physiology*. 2015;119(5):541–557. doi:10.1152/japplphysiol.01133.2014.
117. Lewis CL, Ferris DP. Invariant hip moment pattern while walking with a robotic hip exoskeleton. *Journal of Biomechanics*. 2011;44(5):789 – 793. doi:<https://doi.org/10.1016/j.jbiomech.2011.01.030>.
118. Kao PC, Lewis CL, Ferris DP. Invariant ankle moment patterns when walking with and without a robotic ankle exoskeleton. *Journal of Biomechanics*. 2010;43(2):203 – 209. doi:<https://doi.org/10.1016/j.jbiomech.2009.09.030>.
119. Galle S, Malcolm P, Derave W, Clercq DD. Adaptation to walking with an exoskeleton that assists ankle extension. *Gait & Posture*. 2013;38(3):495 – 499. doi:<https://doi.org/10.1016/j.gaitpost.2013.01.029>.
120. Koller JR, Jacobs DA, Ferris DP, Remy CD. Learning to walk with an adaptive gain proportional myoelectric controller for a robotic ankle exoskeleton. *Journal of NeuroEngineering and Rehabilitation*. 2015;12(1):97. doi:10.1186/s12984-015-0086-5.

121. Lenzi T, Carrozza MC, Agrawal SK. Powered Hip Exoskeletons Can Reduce the User's Hip and Ankle Muscle Activations During Walking. *IEEE Transactions on Neural Systems and Rehabilitation Engineering*. 2013;21(6):938–948. doi:10.1109/TNSRE.2013.2248749.
122. Vanderpool MT, Collins SH, Kuo AD. Ankle fixation need not increase the energetic cost of human walking. *Gait & Posture*. 2008;28(3):427 – 433. doi:<https://doi.org/10.1016/j.gaitpost.2008.01.016>.
123. Cenciarini M, Dollar AM. Biomechanical considerations in the design of lower limb exoskeletons. In: 2011 IEEE International Conference on Rehabilitation Robotics; 2011. p. 1–6.
124. Johnson MA, Polgar J, Weightman D, Appleton D. Data on the distribution of fibre types in thirty-six human muscles: An autopsy study. *Journal of the Neurological Sciences*. 1973;18(1):111 – 129. doi:[https://doi.org/10.1016/0022-510X\(73\)90023-3](https://doi.org/10.1016/0022-510X(73)90023-3).
125. Newham DJ, Mills KR, Quigley BM, Edwards RHT. Pain and Fatigue after Concentric and Eccentric Muscle Contractions. *Clinical Science*. 1983;64(1):55–62. doi:10.1042/cs0640055.
126. Geijtenbeek T. SCONE: Open Source Software for Predictive Simulation of Biological Motion. *Journal of Open Source Software*. 2019;4(38):1421. doi:10.21105/joss.01421.
127. Zhang J, Fiers P, Witte KA, Jackson RW, Poggensee KL, Atkeson CG, et al. Human-in-the-loop optimization of exoskeleton assistance during walking. *Science*. 2017;356(6344):1280–1284. doi:10.1126/science.aal5054.